Development of a Method to Assess EAAT1 Transcription Levels in Alzheimer's Disease

Karl Köchert

2007

DIPLOMARBEIT

FROM

KARL KÖCHERT

BORN ON THE 5TH OF MAY 1982 IN BERLIN, GERMANY

01.02.2007

SUPERVISORS:

PROF. DR. B. MICHEEL

DR. P. DODD

POTSDAM UNIVERSITY

FACULTY OF LIFE SCIENCE

INSTITUTE OF BIOCHEMISTRY

IN COOPERATION WITH THE

UNIVERSITY OF QUEENSLAND, AUSTRALIA

Acknowledgements

I am indebted to the families who gave their consent for the collection of the brain tissue —this project would not have been possible without it.

I would like to thank Dr Peter Dodd for the possibility to work in his research group and Dr Justin Ridge for their advice, guidance and encouragement throughout the project. I moreover would like to thank them for their help when editing this manuscript.

My appreciation extends to everyone in the neuroscience laboratory team who gave his or her time and knowledge to help me solve and overcome all the little experimental problems so inherent to science.

Furthermore I would to thank the DAAD for the granting of a scholarship for this project.

Ganz besonders möchte ich natuerlich meiner Familie, vor allem meinen Eltern danken. Ohne Euch wäre so vieles in meinem Leben nicht möglich gewesen. Ihr habt in mir von früh an das Interesse und die Freude am Kennenlernen anderer Länder und Kulturen geweckt. Ich danke Euch für Eure Unterstützung, Ermunterung und Zustimmung, die mir nicht nur diese Diplomarbeit, sondern auch die Projekte in Spanien und Grossbritannien ermöglicht haben.

Statement of Originality

I declare that the material presented in this thesis is my own work and has not been previously submitted in any form for another degree or diploma at any higher educational institution. To the best of my knowledge, this thesis contains no material previously published or written by another person except were due reference is made.

Ich erkläre, dass die vorliegende Arbeit meine eigene Arbeit darstellt und in keiner Form zuvor eingereicht wurde. Von Stellen abgesehen an denen entsprechende Referenzen angegeben wurden, ist der Inhalt dieser Arbeit nach bestem Wissen und Gewissen von keiner anderen Person geschrieben oder veröffentlicht worden.

Karl Köchert

01.02.2007

Contents

List of Figures

List of Tables

List of Abbreviations

Common SI units are not stated.

Aβ	β-amyloid protein
AD	Alzheimer's Disease
ALS	amyotrophic lateral sclerosis
APP	β-amyloid precusor protein
hAPP	human amyloid precusor protein
sAPP	soluble β-amyloid precusor protein
APS	Ammonium Persulfate
BLAST	Basic Local Alignment Search Tool
bp	base pairs
CDS	coding sequence
CNS	central nervous system
cop	copies
C_t	cycle threshold
DEPC	diethylpyrocarbonate
DNA	deoxyribonucleic acid
cDNA	copy DNA
dsDNA	double-stranded DNA
ssDNA	single-stranded DNA
dNTP	deoxyribonucleoside triphosphate
DST	desalted

EAATn	excitatory amino acid transporter number, n=1-5
EAAT1 wt	excitatory amino acid transporter number 1 wildtype
EAAT1 Δ3	excitatory amino acid transporter number 1 skipping exon 3 variant
EAAT1 Δ9	excitatory amino acid transporter number 1 skipping exon 9 variant
e.g.	exempli gratia
EDTA	ethylenediaminetetraacetic acid
F	female
i.e.	id est
kb	kilo bases
kDA	kilo Dalton
M	molar
MS	mass spectrum
OD	optical density
P	probability
PCR	polymerase chain reaction
RT-PCR	Reverse-transcriptase polymerase chain reaction
PAGE	polyacrylamide gel electrophoresis
SDS	sodium dodecyle sulphate
SN	supernatant
SOI	sequence of interest
TAE	Tris-acetate EDTA
TBE	Tris-borate EDTA
TEMED	tetramethylethylenediamine
wt	wild type version of a gene

Chapter 1

Introduction

1.1 Alzheimer's Disease

1.1.1 Etymology and Usage of the Term "Alzheimer's Disease"

In November, 1906, Alois Alzheimer gave a lecture in Tübingen, Germany, describing the case of Auguste Deter, a patient whom he had been treating since 1901 and who had shown loss of short term memory, impaired judgment, decision-making and orientation. When Auguste Deter died on the 9th of April, 1906, Alzheimer dissected her brain - by using staining techniques he was able to prove vast neuronal-loss and formation of protein-plaques in the cerebral cortex[3].

He later published the data on Deters case [4] and in 1911 his colleague Emil Kraeplin named the disease Alzheimer's disease.

Until the 1970s the term Alzheimer's Disease was only used for people who showed so-called *pre-senile dementia*, i.e. cases younger than 65 years whereas the *senile dementia* of individuals older than 65 years was thought to be the natural process of neuronal loss with increasing age [5]. As it became increasingly clear that *pre-senile dementia*- and *senile dementia*-cases show the same symptoms and brain pathology, the term "Alzheimer's Disease" began to be used for individuals of all ages alike. Yet, today the disease is separated in two types, the so-called familial or early-onset AD (onset before the age of 65 years) and the late-onset AD (onset after the age of 65 years). Though the

results for those "types" of AD are the same, the cause for the familial type can be mainly pinpointed to genetic predispositions which is not the case for late-onset AD as will be explained below.

1.1.2 Epidemiology

A recent study estimates that about 24 million people worldwide suffer from dementia and that this amount will double every 20 years to 81 million by 2040 [6]. The prevalence of dementia grows exponentially with increasing age: in developed countries of the Western World only 1% of individuals having dementia are aged 60-64 years whereas up to 33% of individuals aged 85 years and older suffer from it. AD accounts for approximately 50-60% of all dementia cases [5]. With the proportion of elderly people increasing from year to year it already is, and will increasingly become, a major issue in society for which methods for prevention, early diagnosis and therapy are needed.

1.1.3 Clinical Features

The symptomatology of AD consists of progressive impairment of episodic memory, aphasic, apraxic and agnosic skills. Those symptoms go along with general cognitive symptoms as for example impaired judgment, decision-making, and orientation [5]. As those symptoms may be found in other types of dementia as well, definitive confirmation of AD can only be made after the histopathological examination of post-mortem brain tissue.

It is characteristic for AD, that specific areas of the brain are affected as for example the midtemporal, frontal, caudal cingulate, and hippocampal cortices whereas others like the occipital and motor cortices are spared.

1.1.4 Pathogenesis

Alzheimer already observed that the histopathological hallmarks of AD that are the now so called neurofibrillary tangles (NFTs) and senile/neuritic plaques (NPs) go along with neuronal and synaptic atrophy in medial temporal lobe structures and cortical areas of the brain [5]. Yet it would take another 70 years to analyse what those structures actually consisted of.

Neuritic Plaques: the β-amyloid Cascade Hypothesis

In 1985 the major component of senile plaques was identified to be the 4 kDa amyloid beta peptide (Aβ)[7]. Two years later it was found to be a cleavage product of amyloid precursor protein (APP) [8]. APP is a trans membrane protein which is encoded on chromosome 21 and features a N-terminal extracellular tail, which contains 28 amino acid residues of the membrane spanning Aβ domain. So far, two cleavage ways are known, in which APP can be processed:

- In the non-amyloidogenic (no Aβ is produced) α-*secretase pathway*, α-secretases cleave the extracellular fragment of APP within the Aβ domain, producing a soluble APP fragment called α-sAPP. Two proteases have been identified so far that act as α-secretases: tumor necrosis factor α converting enzyme (TACE) [9] and ADAM 10 [10]. Both belong to the ADAM family of disintigrin and metalloproteinases.

  After that first cleavage step the so called γ-secretase complex consisting of the proteins presinilin-1 (PSEN1, constitutes the active site [11]), presinilin-2 (PSEN2), nicastrin and APH-1 cleaves the remaining C-terminal fragment. It thereby releases the short, soluble p3 peptide which is made up of the amino acid residues 17 to 40/42 of the former Aβ domain. The remaining APP intracellular domain (AICD) is metabolised in the cytoplasm [5].

- In the amyloidogenic (Aβ is produced) β-*secretase pathway* the integral membrane aspartyl protease β-site APP-cleaving enzyme 1 (BACE1) cleaves APP just before the Aβ domain [12]. Soluble βsAAP is released and the remaining c-terminal end is cleaved by γ-secretase into AICD and Aβ peptides that are heterogenic in size, amino acid sequence and therefore biophysical structure. Only 5% of all Aβ species are made up by the amino acid residues 1 to 42 of the former Aβ domain. This so called Aβ42 is much more likely to aggregate than the vast majority of Aβ species, that are made up of amino acid residues 1 to 40 (and are subsequently called Aβ40) of the former Aβ domain. Studies found moreover, that Aβ42 actually supports

aggregation of other Aβ species by triggering a change in their secondary structure to high β-sheet content [13, 14]. This aggregation first leads to small oligomers which then aggregate to NPs (A process similiar to protein crystallisation).

Both cleavage pathways are used during normal cell metabolism and Aβ is degraded by a set of metallopeptidases [15].

The β-amyloid cascade hypothesis states that an imbalance between production and clearance of Aβ ultimately leads to NPs and thereby to neuronal degeneration and dementia [16]. This hypothesis is supported by findings regarding the familial, early-onset type of the disease which is strongly connected to mutations in APP itself and in proteins involved in APP metabolism. The fact that people with Down's syndrome, having three copies of the APP gene, develop Aβ plaques in early life supports that thesis. Yet, the level of relevance of this is in question as the vast majority of AD cases do not show the mentioned mutations, that lead to familial AD. Furthermore some studies find that there is little correlation between the degree of β-amyloidosis and the degree of neuronal/synaptical loss and dementia [17] and that some normal aged individuals without dementia have as much β-amyloid plaques as typical AD cases [18]. A meta study of Lee et al. in 2004 [19] concluded that NPs represent a disease marker with little specificity and are rather a secondary product than a pathogenic mediator in dementia.

Neurofibrillary Tangles

Shortly after the identification of Aβ as the main component of NPs, hyperphosphorylated τ protein was found to be a major component of the NFTs [20]. τ is an axonal protein that acts as a major regulator of microtubule formation in cells [21] by promoting the assembly and stabilization of microtubules. Six isoforms of τ exist and their phosphorylation is regulated by a set of kinases and phosphatases. Abnormal phosphorylation, i.e. hyperphosphorylation of τ not only leads to loss of τ function but actually renders it to be a toxic agent causing inhibition and disruption of microtubules. It moreover results in aggregation of τ into insoluble fibrils in tangles [22]. All this ultimately leads to neuronal death.

The hyperphosphorylation of τ seems to be due to an imbalance between the activities of τ kinases and τ phosphatases as well as changes in τ confirmation which affect its interaction with these enzymes [22]. The discovery of mutations in the τ gene and their co-segregation with the disease in inherited frontotemporal dementia with Parkinsonism linked to chromosome-17 (FTDP-17) has confirmed that abnormalities in τ protein as a primary event can lead to neurodegeneration and dementia [23]. Yet it is still unknown, whether τ hyperphosphorylation and resulting tangle formation are a cause or a consequence of Alzheimer's disease [5] and other taupathies.

Contribution of Glutamate Excitotoxicity to Alzheimer's Disease

The amino acid glutamate acts as the primary excitatory neurotransmitter in the human brain. Yet, its activity at the synaptic cleft has to be carefully regulated by glutamate reuptake and receptor inactivation, as high concentrations of glutamate are neurotoxic [24, 25, 26]. When this regulation is disturbed it may result in excessive neuronal stimulation which ultimately triggers an enzymatic cascade that leads to cell death [27] of neurons and astrocytes —a typical symptom in AD and dementia in general.

Biochemical studies in human post mortem brain tissue have shown that in AD the high affinity glutamate/aspartate uptake system is 40 to 50% decreased in the frontal, parietal and temporal cortex, [28] areas that are especially affected in AD.

Other findings suggest a correlation between APP and excitotoxicity: Normally, secreted APP protects against glutamate toxicity [29] and regulates the expression of glutamate receptor subunits [30]. Yet in AD, APP products seem to impair the glutamergic system [31, 32].

Summarizing, it can be taken for a fact that glutamate metabolism is altered in AD, resulting in excitotoxic levels of glutamate [33]. Therefore it is of great interest to find out whether this altered glutamate transport is cause or consequence of AD and the systems of glutamate transport and reception are under scrutiny.

1.1.5 Genetic Factors

As mentioned in 1.1.1, there are two subtypes of AD: In early-onset, familial AD mutated forms of amyloid precursor protein (APP) [34], presenilin-1 and presinilin-2 [35, 36] were found to trigger the disease. Yet, those cases only account for about 0.1% of all AD-cases[37]).

For late-onset AD it has been found that the ϵ4 allele of APOE, in which Cys112 is changed to Arg, is associated with the disease [38, 39]. A meta-study reported that APOE ϵ4 heterozygotes are three times more likely to get AD, homozygotes even up to 15 times [40]. APOE encodes for the major cholesterol transporter apoE, but so far no mechanism is established to explain why, in case of the APOE $\epsilon 4$ variant, risk for AD is increased. Whereas studies assessing the possibility that the ϵ4 variant is more prone to form complexes with Aβ than the other variants are rather contradictory, a recently developed model examines the role of apoE as antioxidant:
Comparing the antioxidative potential of the APOE variants ϵ2, ϵ3 and ϵ4 it was found that the lacking Cys at position 112 leads to a deficiency to act as antioxidant [41] and therefore might contribute to neuronal death in AD and dementia in general. This goes well with the fact, that oxidative stress harms every organ system and is especially interesting as Aβ is reported to generate free radicals and lipid oxidation products which can cause further damage and inhibition of important physiological functions [1].

1.2 Glutamergic System

As pointed out above, the formation of NPs and NFTs are common hallmarks in AD cases but they are also found in similarly high amounts in a substantial portion (20-40%) of non-demented individuals [5]. This shows once more that AD is a very compelx, multicausal disease that most certainly can not be pinpointed to just a couple of causes.
The theory, that glutamate excitotoxicity is part of AD has put the glutamergic system under scrutiny in order to assess in how far altered glutamate metabolism is cause, consequence and/or an interconnected part with other physiological alterations (e.g. NPs and NFTs) in AD .

1.2.1 Glutamate in the Central Nervous System

Quantitatively, glutamate represents the most important excitatory neurotransmitter in the central nervous system (CNS) [42]. Its release from the synaptic terminal into the synaptic cleft is triggered by a Ca^{2+}-influx caused by an incoming action potential. Crossing the synaptic cleft by simple diffusion, glutamate may bind to ionotropic glutamate receptors (divided into the subclasses of NMDA, AMPA and kainate receptors [43]) or G-protein coupled metabotropic receptors [1]. As glutamate is not metabolised in the synaptic cleft, the most effective means of regulating the glutamate concentration in the synaptic cleft are transmembranal glutamate transporters.

By regulating the extracellular glutamate concentration, these transporters not only prevent toxic concentrations of glutamate but also take part in the recycling of glutamate through the glutamate-glutamine (Figure 1.1).

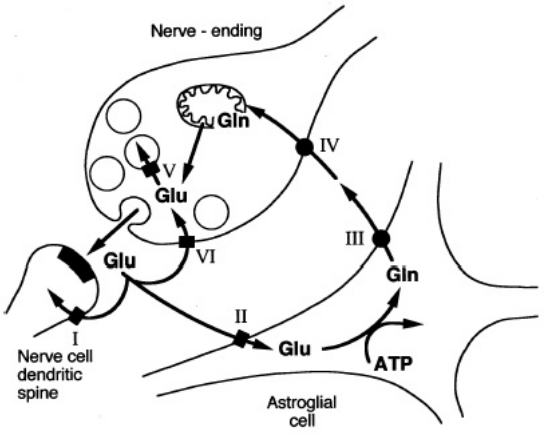

Figure 1.1: The glutamate-glutamine cycle, from [1]

This pathway represents a way of recycling transmitter glutamate. Glutamate released from a nerve terminal by exocytosis is taken up by glutamate transporters present presynaptically (VI), postsynaptically (I) and extrasynaptically in astroglial cells (II). Astroglia detoxifies glutamate by converting it to glutamine. Glutamine is subsequently released from the glial cells by means of glutamine transporter (III) and taken up by neurons by means of other glutamine transporter(IV). Neurons convert glutamine back to glutamate. Synaptic vesicles are loaded with glutamate from cytosol by means of a vesicular glutamate transporter (V).[1]

1.2.2 Na^+-dependent Glutamate Transporters

The best characterized glutamate uptake system is the Na^+-dependent "high-affinity" glutamate transport system. So far, five different human Na^+-dependent glutamate (excitatory amino acid) transporters (EAATs) have been cloned: EAAT1 (synonymous with GLAST in rat), EAAT2 (synonymous with GLT in rat), EAAT3 (synoymous with EAAC in rat), EAAT4 and EAAT5. These five glutamate transporters share 50-60% amino-acid identity with each other and 30-40% with some carriers for neutral amino acids (alanine-serine-cysteine-transporters: ASCT1 and ASCT2) [1].

The transport of substrates by EAATs is an electrogenic process as glutamate-influx is coupled to the cotransport of two or three sodium ions, one proton and the counter-transport of a potassium ion [44]. The transport is therefore driven by an charge-gradient over the plasma membrane which is sustained by Na^+/K^+-ATPases. Thus, sufficient ATP supply is essential for the functioning of the EAATs [45].

Distribution and Relevance of each of the EAATs

Each of the EAATs is distributed differently throughout different tissues:
EAAT1 is expressed and located in the plasma membrane of astroglial cells throughout the CNS and is also found in other tissues for example in bone [46] and blood (in platelets [47] and fibroblasts [33]). Expressed in the whole CNS, *EAAT2* is the major glutamate transporter in the mammalian forebrain and is especially abundant in the hippocampus, lateral septum, cerebral cortex and striatum [48]. In the CNS so far it has only been found to be expressed in astroglial cells where it is localized in the plasmamembrane [1]. Expression of EAAT2 has also been found in β-cells of the pancreas [49].
EAAT3 is expressed in hippocampus, cerebellum and basal ganglia [1], yet in such low amounts that it is insignificant compared to EAAT1 and EAAT2 [50]. It seems to play a more important role in the kidney where it is found in higher concentrations than in the hippocampus [1]. As opposed to EAAT1 and EAAT2, EAAT3 is expressed in neurons [51] and preferentially localized in the cytoplasm [52].
EAAT4 is found in the forebrain in very low concentrations. It is only expressed in significant levels in the glutamergic Purkinje cells of the cerebellar cortex where it is located in the plasma membrane

[1].

EAAT5 so far has only been detected in retina [53] and therefore is probably not related with any neurodegenerative disorder of the CNS.

EAAT1 and EAAT2 are together responsible for most of the glutamate uptake activity which is attributable to the five EAATs [1]. In order to assess the relation of altered glutamate metabolism to neurodegenerative disorders, EAAT1 and EAAT2 are thus the most important candidates to look at when examining the contribution of altered glutamate transport to altered glutamate metabolism.

1.2.3 Mechanisms of Glutamate Excitotoxicity

Extracellular concentrations of $\approx$0.6 μM glutamate are normal —only slightly higher concentrations of $\approx$2-5 μM are neurotoxic [54]. The excitotoxic effects of high glutamate concentrations are caused mainly by excessive overstimulation of glutamate receptors, that may lead to cell death through following pathological mechanisms:

- Increased Na^+- and Cl^-influx disturbs the osmotic balance of the cell. This leads to H_2O influx and subsequent cell swelling that may ultimately result in necrotic cell death [1].

- Massive Ca^{2+}-influx activates different enzyme cascades. They involve lipases, nucleases, proteases and kinases that can trigger cell lysis [54] and hyper-phosphorylation of for example τ-protein (see 1.1.4).
  Increased intracellular Ca^{2+} concentration also triggers release of arachidonic acid and production of reactive oxygen species (ROS) which inhibit glutamate transporters, initiating a *circulus vitiosus* [55].

- Increased intracellular Na^+ concentration leads to ATP deficiency as the Na^+/K^+-ATPase shows an elevated level of activity. This eventually leads to reversed glutamate transport, i.e. excessive glutamate release that may induce cell death in surrounding cells [45].

- Increased extracellular glutamate concentration inhibits a transmembranal cysteine/glutamate-antiporter (which carries cysteine into the cell in exchange for glutamate [56]). The antioxidant

glutathione (γ-glutamylcysteinylglycine) is produced from cysteine. Thus, low levels of intracellular cysteine lead to low levels of glutathione making the cell more vulnerable to oxidative stress.

1.2.4 The Excitataory Amino Acid Transporter 1 (EAAT1)

Features of EAAT1

The 81.7 kb EAAT1 gene is encoded on chromosome five at location 36,642,446-36,724,193 [57]. Where no alternative splicing takes place, Exons 2 to 10 (positions 245 to 1873 of the mRNA [58]) are translated into the EAAT1 protein which is 542 amino acid residues long. The approximate molecular weight is 59,5 kDa. The functional EAAT1 transporter is supposedly a homooligomer, consisting of two to three non-covalently connected EAAT1 molecules which are held in position within the plasma membrane by different anchoring proteins [1].

The topology of EAAT1 is still being discussed, one proposed scheme is shown in Figure 1.2. Regardless to the actual positioning of the EAAT1 domains which has yet to be determined, mutation experiments have shown that the highly conserved amino acid residues Pro392 to Gln415 (encoded on exon 8) form a domain that is critical for the transporter activity [2].

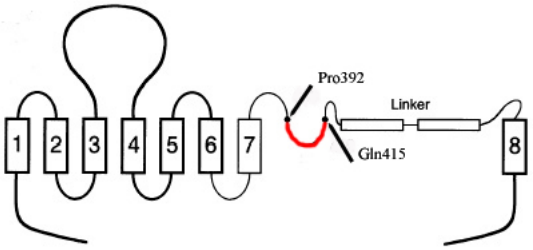

Figure 1.2: Proposed topology of EAAT1, modified from[2]

Numbering represents the trans membrane domains. The highly conserved residues Pro392 to Gln415 are marked red. They form a negatively charged pouch that may therefore be involved in the binding of sodium and/or potassium ions [59].

Alternative splicing of EAAT1

In rat, mRNA for an alternative splice variant of GLAST skipping exon 3 was found [46] and a recent study showed, that it is expressed in rat brain and retina [60]. Moreover, mRNA of an exon 9 skipping variant (EAAT1Δ9) of EAAT1 was found in human brain and the optic nerve. When expressed in HEK293 cells, EAAT1Δ9 is reported to act as a negative regulator of the EAAT1 wt function [61]. This goes well along with the thought that lacking exon 9 would severely change the topology of the peptide sequences encoded for on the neighbouring exons 8 (which is - as mentioned above - probably essential for transporter activity) and 10.

For EAAT2 a couple of splice variants have been found [62, 63]. Due to the high homology of EAATs, it is assumable, that for EAAT1 other splice variants than the found EAAT1Δ9 exist which may take part in normal and/or altered glutamate metabolism.

EAAT1 in Alzheimer's Disease

In transgenic mice expressing hAPP with the London mutation (which is associciated with familial AD) decreased levels of the glial specific glutamate transporters EAAT1 and EAAT2 were observed[64]. Moreover it was found that mice that lack EAAT1 show increased susceptibility to acute cerebellar injury and reduced motor coordination [65], underlining the importance of EAAT1 in glutamate uptake in the normal brain. Another study found that EAAT1 is aberrantly expressed in dementia cases showing Alzheimer-type pathology and proposes aberrant glutamate transporter expression as a mechanism involved in neurodegeneration in Alzheimer's disease [66]. In fibroblasts and platelets of AD cases decreased EAAT1 protein expression and correlation to dementia severity was observed [47, 33]. Splice variants of EAAT2 are associated with amyotrophic lateral sclerosis (ALS) and AD [62], suggesting that the same may apply for splice variants of EAAT1.

Summarizing, one may say that there is strong evidence for an important role of EAAT1 in glutamate excitotoxicity as seen in AD. It is therefore of great interest to assess in which way and to what degree the transscription of the EAAT1 gene, mechanisms of alternative splicing, the subsequent translation and possible posttranslational modifications may lead to altered EAAT1 activity in Alzheimer's dis-

ease.

1.3 Aims and Hypothesis to be Tested

1. Detection of EAAT1 splice variants with focus on the $\Delta 3$ variant reported for rat[60].
2. Establishment of a method using SYBR® Green real-time RT-PCR to quantify mRNA of EAAT1 wt, EAAT $\Delta 9$ and any newly found variant.
3. mRNA quantification of EAAT1 variants including the wt in a set of control-, and AD cases in brain-areas differently affected in Alzheimer's Disease.
4. Assessment of the accuracy and reproducibility of the developed quantification method.
5. Comparative analysis of the transcription rate of all found EAAT1 variants in a set of controls and AD cases:

    - *It is hypothesised that the transcription of the EAAT1 wt and its splice variants is different in Alzheimer's disease. Those disease mediated alterations are partly responsible for neuronal death observed in AD.*
    - *It is moreover hypothesised that there are no different transcription patterns of any of the EAAT1 variants between male and female cases.*
    - *If EAAT1 transcription is a basic cause of AD, its transcription is expected to be significantly different in brain areas that are affected in AD.*
    - *If - as recently suggested [61] - EAAT1 $\Delta 9$ protein acts as a negative regulator of EAAT1 wt function, thereby contributing to the causes and effects of AD, its rate of transcription is expected to be significantly different in AD cases.*

Chapter 2

Materials and Technical Equipment

2.1 Chemicals

item	supplier
Agar	Astral Scientific
Agarose, DNA grade	Quantum Scientific
Ammonium Persulfate	Sigma-Aldrich
Acrylamide/Bis (29:1) 40%	Sigma-Aldrich
Boric Acid	MERCK
Bromphenol Blue	
dNTPs	Promega
Ethanol 99.8%	UQ Chemical Store
Ethidium Bromide (10 mg/ml)	Progen
Ethylenediaminetetraacetic Acid Di-Sodium Salt (EDTA)	Ajax Finechem
Formamide	Amresco
Glacial Acetic Acid	Ajax Finechem
Glycerol	Ajax Finechem
Glucose	Ajax Finechem
isopropyl3-D-thiogalactopyranoside (IPTG)	Sigma-Aldrich

$MgCl_2$	Sigma-Aldrich
NaCl	Ajax Finechem
Sodium Acetate	MERCK
Sodium Dodecyl Sulfate	Bio Rad
Sucrose	Ajax Finechem
Oligonucleotides	Sigma-Genosys
Phenol	Sigma-Aldrich
Phenolchloroform-isoamyl alcohol mixture pH 7.9 (49.5:49.5:1)	Sigma-Aldrich
N,N,N',N'-tetramethylethylenediamine (TEMED)	Sigma-Aldrich
Trizma® Base	Sigma-Aldrich
Tryptone	Beckton Dickinson and Company
DNase/Rnase free water	Gibco
5-bromo-4-chloro-3-indolyl-beta-D-galactopyranoside (X-Gal)	Sigma-Aldrich
Xylene Cyanol FF	Ajax Finechem
Yeast Extract	Beckton Dickinson and Company

2.2 Buffers and Media

GYT medium:	10% Glycerol; 0.125% yeast extract; 0.25% tryptone
LB Medium:	1.0% tryptone; 0.5% yeast extract; 1.0% NaCl adjusted to pH 7.0 with NaOH
Loading Buffer for gel electrophoresis:	0.25% (w/v) bromophenol blue; 0.25% (w/v) xylene cyanol FF and 15% (w/v) Ficoll in water
TE-buffer:	10 mM Tris-HCl; 1 mM EDTA; pH 5.2
1x TAE-buffer:	0.04 M Tris-acetate; 0.001 M EDTA
1x TBE-buffer:	0.045 M Tris-borate; 0.001 M EDTA
PAGE elution buffer:	0.5 M $CH_3COOHNH_4$; 1 mM EDTA
Sequencing buffer:	400 mM Tris pH 9.0; 10 mM $MgCl_2$
SOC-Medium:	0.5% Yeast extract, 2.0% tryptone, 10mM NaCl, 2.5mM KCl, 10mM MgCl2 , 20mM MgSO4, 20mM glucose

2.3 Cell Lines, Vectors and Antibiotics

Ampicillin	Sigma-Aldrich
E.coli XL-Blue cell line	Stratagene
pGEM®-T Easy Vector	Promega

2.4 DNA Molecular Weight Markers

1 kb DNA Step Ladder	Invitrogen
100 bp DNA Step Ladder	Invitrogen
25 bp DNA Step Ladder	Promega

2.5 Enzymes and PCR Reagents

AmpliTaq Gold® 5 U/μl, including buffers	Applied Biosystems
Elongase® Enzyme Mix, including buffers	Invitrogen
Rnase H	Invitrogen
RNaseOUT^{TM} Ribonuclease, 40 U/μl	Invitrogen
SuperScript^{TM} III Reverse Transcriptase, 200 U/μl	Invitrogen
T4 DNA Ligase, 3 Weiss/μl	Promega
SYBR® Green PCR Master Mix	Applied Biosystems

2.6 Kits

pGEM®-T Easy Vector System	Promega
PureLink^{TM} HiPure Plasmid DNA Purification Kit	Invitrogen
Wizard® PCR Clean up System	Promega

2.7 Used Software

ABI Prism 7000 SDS Software 1.1	Applied Biosystems
ABI Prism SDS Software 2.2.2	Applied Biosystems
BioEdit Sequence Alignment Editor 7.0.5.3	Tom Hall
BLAST 2.2.15	Altschul S.F.
OligoAnalyzer 3.0	Integrated DNA Technologies

2.8 Technical Equipment and Consumable Material

ABI 7000 Sequence Detection Syatem	Applied Biosystems
ABI 7900 Sequence Detection System	Applied Biosystems
Auctoclave ES-315	Tomy
Balance "Explorer"	Ohaus
Centrifuge "J2-21" with JA-10 and JA-20 rotors	Beckman
Electrophoresis Equipment for PAGE- and Agarosegelelectrophoresis	BioRad
Electroporation System "MiniPulser"	Biorad
Incubator	MEMMERT
Heater and stirrer "Cimarec®"	Thermolyne
Master Cycler PCR Machine	Eppendorf
Microwave	LG
Peltier Thermal Cycler PTC-200	MJ Research
Pipettes (P2, P10, P200, P1000)	Gilson
pH Meter "HI9321"	Hanna Instruments
RNase and DNase free reaction tubes (0.2, 0.6, 1.5 and 2 ml)	Quality Scientific Plastics
RNase and DNase free filtered pipette tips (10, 20, 200 and 1000 μl)	Quality Scientific Plastics
Tabletop centrifuge "5415C"	Eppendorf

Chapter 3

Methods

Material used in the methods described below such as pipette tips, tubes, centrifuge bottles, glass-ware, water, media and so forth were autoclaved at 121°C for 20 min to ensure sterility.

When DNA/RNA sequences are mentioned below, the numbering of positions is relative to the 5'-end of the sense strand.

3.1 Sample Collection and Preparation

Authorized pathologists performed autopsies with full macroscopic and microscopic examinations to confirm disease diagnosis. The brains were cut into left and right hemispheres, one half was preserved in formalin for further pathology whereas the other half was dissected. Pieces of different brain regions were taken, slowly frozen in 0.32 M Sucrose and stored at -80°C. The brain areas listed below were examined in this project and chosen so because they are differently effected in AD. This was used as an internal control for the experiments done in this project as to determine whether any effect observed is specific for AD, i.e. AD affected areas or is generally seen in all areas examined.

- Inferior Temporal - is effected in AD
- Inferior Frontal - is effected in AD

- Posterior Motor - little effected in AD
- Occipital Pole - little effected in AD

Post mortem intervals, clinical history and cause of death were noted and a detailed brain autopsy report was provided by the appointed pathologist.
In this project, 12 controls and 11 AD cases made up the case-set to be examined. A listing of all cases may be found in table 6.1.

3.2 total-RNA Extraction from Brain Tissue

About 0.5 g of frozen brain tissue was cut in the cold room and immediately put into a 15 ml falcon tube on dry ice. The following steps were all done in the fume hood to avoid contamination: The tissue was weighed and 10 ml Trizol® reagent per 1 g tissue was added. Trizol® is a mono-phasic solution of water saturated phenol and guanidine isothiocyanate. The latter is a strong denaturing agent that disrupts protein structure wheras the watersaturated phenol acts as solvent for the rather lipophilic proteins and the hydrophilic nucleic and ribonucleic acids. The solution was homogenized immediately using the polytron until it showed a smooth creamy consistency. Incubation for five minutes at RT was allowed followed by the addition 0.2 ml chloroform per 1 ml Trizol reagent to the solution which was then shaken vigorously and incubated at RT for 3 min. The solution was centrifuged at 10 000×g for 20 min at 4°C, resulting in the separation to a three-phase system: Proteins are only found in the organic bottom layer, DNA is to be found in the interphase and RNA is only to be found in the aqueous phase which was transferred to a fresh tube. Isopropanol (0.5 ml per 1 ml Trizol) was added to precipitate the RNA and the solution was centrifuged at 10 000×g for 15 min at 4°C. The SN was decanted and the RNA-pellet resuspended in 75% Ethanol for washing. The solution was centrifuged at 12 000×g for 20 min at 4°C to pellet RNA again and was then allowed to dry at RT in the fume hood for 2-3 hours. The pellet was then resuspended in DEPC treated water and stored at -80°C for further use.

3.3 Preparation of Electrocompetent Cells

The following protocol was used to prepare a stock of electrocompetent cells for transformation with a vector:

1. A single colony of *E.coli* XL-Blue strain was taken from a fresh agar plate and used to inoculate 50 ml LB medium (containing streptomycin, 100 μg/ml). The culture was incubated over night at 37°C/250 rpm.
2. The over night culture was used to inoculate 250 ml LB cultures (1:100 dilution of the over night culture) in 1 L flasks. Incubation at 37°C/250 rpm followed —OD_{600} was measured every 30 min.
3. At OD_{600}=0.4 flasks were placed on ice and chilled for 30 min.
4. Cultures were decanted in chilled centrifuge bottles and cells were harvested by centrifugation (3000$\times$g, 15 min, 4°C). Supernatant was discarded.
5. Cells were resuspended in 500 ml ice-cold water. Cells were harvested as above and supernatant was discarded.
6. Cells were resuspended in 250 ml ice-cold 10% glycerol. Cells were harvested as above, supernatant was discarded.
7. Cells were resuspended in 10 ml ice-cold 10% glycerol and transfered to chilled 50 ml tubes. Cells were harvested as above, supernatant was discarded..
8. Cells were resuspended in 1 ml ice-cold GYT medium.
9. OD_{600} was measured of a 1:100 dilution of the cell suspension. Cell concentration was adjusted to ca. 2.5×10^{10} OD_{600} of 1$\approx$$2.5\times10^{8}$ cells).
10. Conductivity was measured by electroporating 40 μl of the cells. Cells were washed again in GYT medium if arcing occurred.
11. Cells were aliquoted into tubes in 110μl aliquots, snap frozen in liquid nitrogen and then stored at -80°C.

3.4 Gel Electrophoresis

Agarose gels and polyacrylamide gels were used in this project to separate DNA according to its size. When an electric field is applied to a gel matrix, dsDNA (due to its negatively charged phosphate backbone) will migrate through it towards the anode at rates that are inversely proportional to the $\log_{10}$ of the number of base pairs. Different concentrations of different polymers are used depending

on the size of the DNA fragments that are to be separated, the amount of the DNA and the desired resolution of separation (rule of thumb: the higher the polymer concentration, the higher the resolution).

3.4.1 Agarose Gel Electrophoresis

Agarose gel electrophoresis was used most of the times during this project when DNA had to be separated according to its size. Agarose is a linear carbohydrate (made up of β-D-galactopyranose-(1->4)-3,6-anhydro-L-galactopyranose units) polymer of an approximate molecular weight of 120 000 g/mol. A gel matrix was produced by dissolving the appropriate amount of agarose powder in 1$\times$TAE buffer (by heating in a microwave and subsequent stirring) to get the desired polymer-percentage (w/v) —2% agarose gels were used to sepertae DNA fragments between 300 and 2000 bp long, for fragments shorter than 300 bp 3% gels were used. The gel was cooled down to about 50°C, ethidium bromide was added (0.04 μl per 1 ml of gel matrix) and the gel poured in the gel tray held by the casting stand. The gel was allowed to set and cool down for at least 30 min. The samples were mixed with loading buffer (8:10 ratio), loaded into the wells, one well was loaded with DNA molecular weight marker that would cover the range of fragment-sizes expected within the samples. Gels were run in 1$\times$TAE buffer at 100 V until the bromophenol blue band of the loading buffer had run down approximately two thirds of the gel. Ethidium Bromide binds to dsDNA and fluoresces orange when excited with UV light (absorption maximum of the dsDNA-Ethidium Bromide complex is about 254 nm [67]). DNA bands on the gel were vizualized on a UV light box and photographed.

3.4.2 Polyacrylamide Gel Electrophoresis (PAGE)

Polyacrylamide is the polymerization product of acrylamide monomers linked by N, N'-methylenbis-acrylamide in a free radical addition reaction started by radicals. The radicals are provided by ammonium persulfate and stabilized through hyperconjugation by the sp^3 hybrid orbitals of the methyl-

groups of TEMED.

The length of the chains is determined by the concentration of acrylamide in the polymerization reaction. The resolution of the gel is then a function of chain length[68].

PAGE electrophoresis was used in this project only when the following advantages of this type of DNA seperation were needed [68]:

- The resolution of PAGE is much better than that of agarose gels. It is possible to seperate DNA fragments that differ 0.2% in length.
- It is possible to accomodate much larger quantities of DNA than on agarose gels.
- DNA recovered from polyacrylamide gels is extremely pure.

.

Nondenaturing PAGE

Nondenaturing PAGE was used in this project to seperate DNA fragments when high resolution was needed to analyze the products of the PCR products when amplifying the full EAAT1 CDS (see section 3.8.1). The expected products had a putative size 1000 to 1700 bp and therefore 3.5% polyacrylamide gels were used for seperation. For each 100 ml of 3.5% polyacrylamide gel the following was mixed together:

- 8.75 ml Acrylamide/Bis (29:1) 40%
- 69.85 ml H_2O
- 20.00 ml 5xTBE
- 0.70 ml 10% (w/v) Ammoniumpersulfate

After those reagents were thoroughly mixed, 35 μl TEMED was added and the gel cast immediately between two glass plates held apart by 0.75 mm spacers, fixed to the casting stand. The desired comb was inserted and the gel was left to polymerize for 60 min. The wells of the gel were then flushed with running buffer ($1\times$TBE), the loading procedure and running conditions were the same as the one described for agarose gel electrophoresis. After the run the gel was put in 50 ml water with 5 μl of

ethidium bromide solution and put on a shaker for 30 min. Visualization of DNA was then done on a UV light box.

Denaturing PAGE and Primer Purification

This technique was used for the purification of some primers used in real-time PCR in order to separate the full length primer from degraded, shorter primers which are prone to nonspecificity. It resembles the method described for nondenaturing PAGE with the exception that urea as denaturing agent was added to the gel solution to a final concentration of 7 M to totally dissolve any secondary structure of the primers when running in the gel. The samples were mixed 1:1 with formamide and incubated at 60°C to dissolve secondary structure and then immediately loaded onto the wells and run at 200 V for 90 min. Visualization of DNA was done by ethidium bromide staining.

As the brightest band normally represents the full length primer (whose proportion is supposedly the biggest within the mixture of full length-, degraded primers and partially protected primers [69]) it was excised using a scalpel blade. The gel matrix was cut in little pieces which were put in PAGE elution buffer in a tube. The tube was put in liquid nitrogen to snap freeze its contents and then quickly thawed by incubation at 90°C for 5 min. This procedure helps to disrupt the gel matrix and allows more effective diffusion of the primers from the gel matrix into the PAGE elution buffer. The gel pieces were left in the elution buffer over night and the elution buffer was then pipetted into a new tube. The primer was then EDTA/EtOH precipitated (see 3.7) and the resulting pellet was dissolved in DNase/RNase free water.

3.5 Storage of Bacteria

To create a stock of a clone, bacteria were grown over night in LB medium (with an appropriate antibiotic) at 37°C, shaking at 150 rpm. Thereafter, 150 μl of the grown culture were put in a 1.5 ml tube, mixed with 850 μl of glycerol and shock-frozen in liquid nitrogen. Bacteria were stored at -80°C until further use.

3.6 Isolation of Plasmid DNA from bacteria

For the isolation of plasmid DNA amplified in *E.coli* XL-Blue, the PureLink^{TM} HiPure Plasmid DNA Purification Kit was used according to the provided manual. Cells were grown over night in LB medium (0.1 mg Ampicillin/ml) at 37°C, shaking at 150 rpm and then lysed under alkaline conditions. The principle of the following plasmid DNA purification is based on the usage of an anion-exchange column to which the negatively charged phosphate-backbone of DNA and RNA binds. Binding is a function of temperature, salt concentration, pH, DNA/RNA size and secondary structure. Under moderate salt conditions plasmid DNA remains bound to the column whereas the bacterial genome, RNA, proteins, carbohydrates and other impurities are washed away with low-salt washing buffer. The plasmid DNA can then be eluted from the column using high-salt buffer and is further purified by simple Isopropanol/EtOH precipitation [70].

3.7 DNA Clean up Methods

Being a highly polar species, DNA is easily soluble in polar solvents like H_2O. Its solubility decreases with increasing apolarity of the solvent, with increasing concentration of highly soluble species like salts within the solvent (solubility products are different for each species) and with decreasing temperature of the solvent. Most of the DNA purification methods are based on those characteristics of DNA and there are many different ways to do it , depending on what is to be separated (e.g. salt, proteins, carbohydrates) from the DNA, what volume it is to be precipitated from etc..

In this project, the *EDTA/EtOH precipitation* method was used to clean up the product of the sequencing reaction. As capillary electrophoresis and subsequent fluorescence detection was used to analyze the products of the sequencing reaction(see 3.11.2) it is imperative to eliminate any kind of impurity, especially salt which would interfere with the resolution of the capillary electrophoresis. For this purpose EDTA was added to a final concentration of 30 mM to bind metal ions from the sequencing reaction (Mg^{2+}) and EtOH was added to a final percentage of 70%. This was mixed gently and incubated at room temperatue for 20 min allowing the DNA to percipitate wheras the EDTA-bound

ions stay in solution. The precipitated DNA was then centrifuged down 14000 rpm for 30 min, the supernatant decanted and the pellet washed with 70% EtOH to wash away remaining salt and other impurities. The DNA was again sedimented at 14000 rpm for 30 min in a tabletop centrifuge, the supernatant decanted and the pellet dried at 37°C in an incubator.
For the clean up of normal PCR products that were to be used for cloning (see 3.11), the *Wizard®* *PCR Clean up System* was used according to the supplied manual[71].

3.8 Primer Design

All primers designed in this project were bought DST-purified from Sigma Genosys. A list of all primers used and their characteristics may be found in table 6.2.

3.8.1 Primer Design for Amplification of the EAAT1 CDS

The mRNA sequence #NM_004172 of EAAT1 was obtained from the NCBI database [58]. The EAAT1 mRNA consists of 3983 bases, the CDS reaches from position 245 to 1873. The aim was to PCR-amplify the whole CDS in order to screen the products for possible EAAT1 variants and to clone them into a vector to produce a standard for mRNA-quantification. Therefore primers were designed to amplify the full CDS: EAAT1 CDS FP covers positions 245 to 269 and EAAT1 CDS RP positions 1851 to 1873 of the EAAT1 mRNA.

To ensure specificity of the primers - according to a rule of thumb - they should be at least 16 bases long. As the EAAT1 mRNA is very similar to the mRNAs of the other EAATs in human, the primers were designed to be 25 and 23 bases long as for the forward primer and the reverse primer, respectively. The sequences were then analysed in regard to possible homology to DNA- and mRNA-sequences to be found in human using the BLAST program and were found to be only present in the actual EAAT1 mRNA sequence.
Moreover both primers were designed in a way that they would have approximately the same GC-content and length and therefore similar annealing temperatures. The Oligo Analyzer 3.0 from Integrated DNA Technologies was then used to assess theoretical annealing temperatures of the primers,

possible formation of primer dimers, of secondary structures and their melting temperature (which should be beneath the annealing temperature).

3.8.2 Primer Design for the Detection of the EAAT1 $\triangle$3 and $\triangle$9 Variants in cDNA Samples Transcribed from Total RNA Extract of Control Cases

To detect EAAT1 variants that lack exon 3 or exon 9, primers were designed that amplify a sequence part of the EAAT1 mRNA that starts in exon 2 and ends in exon 4 and a sequence that starts in exon 8 and ends in exon 10. The resulting PCR product was then to be analysed by gel electrophoreses - differently sized bands are expected for the wt and exon-skipping amplicons, respectively. Table 3.1 shows a summary of the characteristics of the designed primers and the expected size of the wt amplicon and the exon-skipping amplicons. Primers were subjected to the tests described above in section 3.8.1.

Table 3.1: Primers used for the Detection of EAAT1 wt, EAAT1Δ3 and EAAT1Δ9.
Primers were used for detecion of the variants in cDNA samples from human brain tissue and in PCR-Colony-Screening(section 3.11.1).

Primer Pair	amplified region	expected amplicon-size for wt [bp]	expected amplicon-size for exon 3 skipper [bp]	expected amplicon-size for exon 9 skipper [bp]
EAAT1 exon 2a FP, EAAT1 exon 4 RP	exons 2 to 4	282	157	282, not distinguishable from wt
EAAT1 exon 8 FP, EAAT1 exon 10 RP	exons 8 to 10	358	358, not distinguishable from wt	223

3.8.3 Primer Design for the SYBR® Green Real-Time PCR Quantification of EAAT1 wt, EAAT1Δ3 and EAAT1Δ9 mRNA

In order to quantify EAAT1wt, EAAT1 Δ3 and EAAT1 Δ9, primers had to be designed that specifically and only amplify either one of the variants. To achieve this, either the forward or the reverse primer was designed in a way that it would cover an exon-exon boundary that only exists in the EAAT1 variant that is to be quantified. Primer design was therefore restricted to very short parts of the EAAT1 sequence. The percentage of bases that are overlapping the junction at the 3'-end of

the primer has to be carefully balanced because the 3'-end is the binding site of the polymerase and therefore essential for the specificity of the primer. If the 3'-end of the primer is overlapping too many bases unspecific priming may occur on other sites of the templates which are complementary to the short overlapping sequence at the 3'-end. If the overlapping 3'end is too short though, unspecific priming may occur as well as the polymerase is able to override one to two mismatching bases at the 3'end (this is empirically proved by usage of mismatch primers for the introduction of mutations and/or restriction enzyme cleavage sites). As primer binding is a very complex thermodynamical process, only empirics provide a way to determine whether a theoretically specific primer really features enough specificity for the needs of an experiment.

For this project, different variants of the exon-exon-boundary spanning primers were designed that featured overlapping 3'-ends of $\approx$5% to $\approx$42% of the whole primer length. All primers to be used in the Real-time-PCR quantification were designed to give amplicons of about 200bp length, having annealing temperatures of around 58^{o}C. The tests described in section 3.8.1 were done and special attention was paid to avoid possible formation primer dimer as this would give an unwanted background signal in the real-time-Quantification as the fluorescent dye SYBR® Green binds to any dsDNA. Figure 3.1 shows schematically how primers were arranged.

The EAAT1 wt was to be determined at two different positions of its sequence as shown in figure 3.1. The primer pair amplifying the wt exon 2-4 area will not only amplify the wt but will also amplify the EAAT1 Δ9 variant as it has the same sequence in the exon 2-4 area. The named primer pair will therefore quantify the sum of the wt and the Δ9 variant. As the latter is quantified separately the quantity of the wt may be calculated by subtracting the determined amount of the Δ9 variant from the sum of the determined quantity of EAAT1wt+EAAT1 Δ9.

The same principle goes for the primer pair amplifying the wt and Δ3 exon 8-9 areas. Again, the actual quantity of wt may be calculated by subtracting the determined quantity of EAAT1 Δ3 from the sum of EAAT1wt+EAAT1 Δ3.

The reason for amplifying the wt at two different positions was to assess the reproducibility of the method used to quantify all EAAT1 variants when different experimental conditions were applied

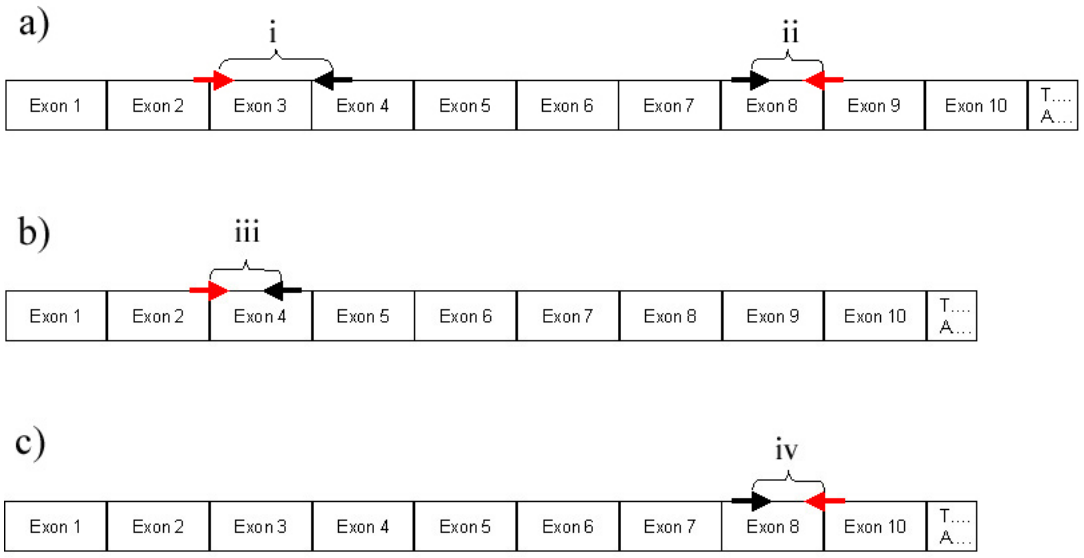

Figure 3.1: Scheme of the cDNA structure of possible EAAT1 variants

Shown are cDNA schemes of a) EAAT1 wt, b) EAAT1Δ3 and c) EAAT1Δ9. Approximate location of primer pairs designed to amplify specifically i) exon 2-4 area of EAAT1 wt, ii) exon 8-9 area of EAAT1 wt, iii) exon 2-4 area of EAAT1Δ3 and iv) exons 8-10 area of EAAT1Δ9 are marked. Exon-exon-boundary spanning primers are coloured red.

—the determined quantity of the wt amplified in two different areas of its sequence are theoretically the same. Differences in the measured quantities between both sequence parts would then give an estimate of accuracy and reproducibility of the method.

3.9 PCR

The standard polymerase chain reaction (PCR) technique was used throughout the whole project and allows the amplification of DNA. By designing oligonucleotides (primers) that are complementary to a specific region on the sense and anti-sense DNA strands, respectively, it is possible to amplify a specific DNA fragment. A DNA Polymerase (in my experiments usually AmpliTaq Gold®, derived from *Thermus aquaticus*) is used for the amplification of the desired DNA-fragment. Desoxynucleotidetriphosphates (dNTPs) at a concentration of 250 μM for each type (dATP, dCTP, dGTP, dTTP), $MgCl_2$ in a concentration range of 1.0 to 4.0 mM and PCR-buffer provided with the *Taq* polymerase were used with about 100 ng of template DNA for the amplification. The PCR-buffer adjusts the pH and the

ionic strength to an optimum for the polymerase whereas the $MgCl_2$ is needed because Mg^{2+} binds to the phosphate-residues of the dNTPs which only then can be used by the polymerase. Moreover Mg^{2+}-concentration contributes to the just mentioned ionic strength but more importantly influences the structure of the primers, the template DNA and the produced amplicon and therefore the melting temperatures of those molecule's secondary structure, if they have any.

The standard PCR consists of the following steps which are realized in a thermocycling machine:

1. *Denaturing of the dsDNA:* The reaction mixture is kept at 95°C for 1 to 10 min to assure complete denaturation of dsDNA (i.e. the breaking of the hydrogen bonds between complementary strands) which is important for the next step.
2. *Annealing of the Primers:* the temperature is lowered to allow the annealing of the primers to their complementary sequence on the template DNA.
3. *Elongation:* the temperature is elevated to 72°C which is the temperature optimum for *Taq* polymerase. The Enzyme binds to the primer-template complex and starts complementing the DNA strand in 5'-3' direction. This step takes about 30 seconds per 500 base pairs.

Steps 1 (though step one is shortened to about 30 s, as by then this time is sufficient to melt any newly formed dsDNA) to three are now repeated for 30-40 times and then followed by a final elongation step of about 10 min to ensure that any remaining single strand DNA is copied.

3.9.1 Temperature Gradient PCR

Whenever a newly designed primer was used for the first time a temperature gradient PCR was done to check the theoretically calculated annealing temperatures and if there were any better temperatures regarding primer specificity and DNA yield. The gradient machine used is capable of running a normal PCR-program while putting each sample to a specific annealing temperature during the Primer-Annealing step. Usually temperature gradients were run that used different annealing temperatures of ± 4°C around the theoretically calculated annealing temperature.

3.9.2 Reverse-Transcriptase PCR

In order to quantify EAAT1 mRNA, total RNA-extracts from human brain tissue of different areas were transcribed to cDNA, using Reverse Transcriptase-PCR. This was done according to a highly standardized protocol to keep different samples comparable when doing the quantification by means of SYBR® Green Real-Time PCR.

Oligo (dT)15, random hexamer primers and SuperScript III Reverse Transcriptase were used to translate virtually every mRNA, that may be in the total RNA extract. The obvious advantage of using cDNA to analyse the features of the RNA it was transcribed from is its better stability and the possibility to amplify it easily in any standard PCR as to gain a product that can be used for genotyping, detection of splice variants, cloning etc.. The following protocol and the SuperScript III Reverse Transcriptase System from Invitrogen was used for RT-PCR:

- 3 μl of total RNA extract (1 μg/μl)1 μl 10 mM dNTPs
- 2 μl Oligo (dT)15 primer (500 μg/ml)
- 1 μl random hexamer primer (500 μg/ml) 5 μl ddH2O were added in a RNAse/DNAse free tube and incubated at 65°C for 5 min.
  Thereafter,
- 4 μl of Buffer A
- 1 μl 0.1 M DTT
- 1 μl RnaseOUT^{TM}
- 1 μl SuperScript III Reverse Transrciptase

were added and subsequently subjected to the following temperature program:

1. Incubation at 25°C for 5 min
2. Incubation at 50°C for 60 min
3. Incubation at 70°C for 15 min

Afterwards 1 μl of Rnase H was added followed by incubation at 37°C for 20 min to degrade any remaining RNA to gain cDNA free of RNA contaminations that could interfere with follow-up experiments that were to be done with the cDNA.

3.9.3 PCR with Elongase® Enzyme Mix

Whenever DNA is to be cloned and then used for e.g. protein expression it is of utter importance, that the DNA sequence is correct. *Taq*-polymerase however is lacking proof-reading-capability and has a error rate of about one in 10.000 amplified base pairs. The Elongase® Enzyme mix-system consists of a mixture of *Taq* and *Pyrococcus*- species thermostable DNA polymerases, containing a proofreading enzyme. PCR-products produced by using this enzyme mixture are therefore nearly 100% complementary to their original template and may be therefore used for cloning and subsequent expression work - nevertheless the cloned inserts have to be sequenced to be absolutely sure that they contain the sequence of interest.

3.10 A-tailing Reaction of Elongase® Enzyme mix-PCR Products

The pGEM®-T Easy Vector System used in this project (see section3.11) features a linearized vector with two sticky ends that are made up by one overlapping deoxythymidine at each end. To clone an insert in this vector it is therefore necessary to create a PCR-product with an overlapping deoxyadenosine at each end.

This is done by the so-called A-tailing reaction which takes advantage of the characteristic of *Taq*-polymerase to extend DNA with an overlapping deoxyadenosine. The reaction is basically a one-temperature-one-step procedure where the *Taq*-polymerase works under the usual PCR-conditions (regarding $MgCl_2$-concentration etc.) with the exception that the only nucleotide triphosphate used is dATP in a final concentration of 0.2 mM.

The protocol used for the A-tailing reaction was taken from the pGEM®-T Easy Vector System-Manual and is as follows:

1. 1-7 μl of purified PCR product generated by Elongase® Enzyme mix are taken and 1 μl 10x PCR-buffer and 1 μl 25 mM $MgCl_2$ were added

2. 5 U of *Taq*-polymerase were added

3. Deionized water was added to a final volume of 10 μl

4. Incubation at 70°C for 30 min

3.11 Standard Construction for mRNA Quantification of EAAT1 Variants: Cloning of EAAT1 Variants

The full length CDS of EAAT1 was amplified with Elongase® Enzyme mix - PCR with the primers mentioned in section 3.8 using total cDNA from control cases as template. The PCR product therefore contains DNA-amplicons of the EAAT1 wt and all possible splice variants that may have been in the original cDNA template. After purifying it with the Wizard® PCR Clean up System, the PCR-product was subjected to an A-tailing reaction as described in 3.10 and the product was subsequently used in a ligation reaction with the pGEM®-T Easy Vector System (map of the vector to be found in Figure 6.1). As proposed by the supplied system manual [72], different insert-vector ratios were tried in the ligation reaction. The setup for the 10 μl standard ligation reaction was as follows:

- 5 μl 2x Rapid Ligation
- 1μl pGEM®-T Easy Vector (50 ng/μl)
- 3 μl purified PCR product
- 1 μl T4 DNA Ligase (3 Weiss)

were mixed by pipetting, incubated for one hour at room temperature and then over night at 4°C. Subsequently 2 μl of the ligation product were mixed with 50 μl of *E. coli* XL Blue-strain (OD≈1) and put on ice for 30 min to allow the ligation-product to adsorb onto the cell surface. Cells were then electroporated (conditions: 25 μF, 200 Ω, 2.48 kV), immediately mixed with 950 μl of pre-warmed (37°C) SOC-Medium and put into an incubator for 1 hour, shaking at 150 rpm and 37°C. Cells

where then centrifuged at 3500 rpm for 5 min in a table-top centrifuge. Most of the supernatant was decanted and the cells resuspended in the rest of the supernatant. Cells were then spread out on a LB-Agar plate containing 0.1 mg Ampicillin per ml LB-Agar . The plate was moreover spread with IPTG and X-Gal. The cells were then grown over night at 37°C. Due to the presence of Ampicillin, only cells with the vector - which carries Ampicillin resistance - were able to grow. The presence of IPTG and X-Gal allowed white-blue selection of colonies, where - theoretically - blue colonies would contain the vector without insert and white colonies the vector with the successfully ligated insert as the insertion interrupts the β-galactosidase sequence (β-galactosidase catalyses the hydrolysis of X-Gal into colorless galactose and deep blue 4-Cl-3-Br-Indigo). Yet, for various reasons (see [72]) it is still possible, that blue colonies contain the vector with insert and that white colonies contain only the vector without insert. Single colonies were picked from the plate and spread out on LB-Agar plate with Ampcillin (same concentration as above) and grown over night.

3.11.1 Colony Screening

Classical Colony Screen

The next day about one third of each of the colonies was put in 1.5 ml tubes, mixed with 50 μl of 2% Triton X-100 pH 12.4 and 10 μl of DNA-loading dye and vortexed. Thereafter 50 μl of pre-mixed phenol:chlorform:isoamylalcohol (25:24:1) pH 7.9 were added, followed by vortexing. The tubes were then centrifuged at 14000 rpm for 5 min in a table-top centrifuge. From the DNA-containing top layer, 20 μl were taken and loaded onto a 1%-agarose gel. A 1 kb molecular weight ladder was loaded as well, as to assess the size of the different DNA-fragments within the bacteria. As the vector is circular its actual size can only be estimated to a limited degree of certainty because the used molecular weight ladder consists of linear DNA-fragments. The higher bands on the gel contain the vector plus the insert whereas lower bands only contain the vector plus some kind of smaller insert (e.g. PCR-products that were not fully elongated etc.) or the vector by itself, yet being arranged in a way that the sequence coding for β-galactosidase is interrupted.

Colony Screening using PCR

The classical colony-screening method described above only allows to detect whether the vector contains any kind of insert that is approximately of the size of the sequence of interest. It is therefore imminent to sequence the cloned insert which on the other hand is costly and time consuming. With a PCR-Colony-Screening it is possible to diminish the number of clones that should be subjected to sequencing to a reasonable number. With this technique, primers are used that are designed to be complementary to and to amplify a part of the sequence of interest. A PCR done with material of the colonies and those primers may the result in PCR-products of three categories:

1. No product detectable: There is no insert or the insert is not completely identical with the sequence of interest.
2. Product of the expected size detectable: The primers bind to the insert - as the product is of the expected size this is strong evidence for the insert being identical with the sequence of interest.
3. Product of unexpected size detectable: The primers bind meaning that at least at the primer-binding-sites the insert is identical with the sequence of interest. As the product is not of the expected size the insert is either artificially changed or represents a variant of the sequence of interest.

It is possible to screen batches of colonies and to categorize them according to one of the possible PCR-results described above. Colonies of batches that belong to the category of interest (presumably categories number 2 and 3) may than be analysed separately using the same PCR-procedure as for the batch-screen.

In this project the Colony-Screening-PCR was used to detect clones that either contained the EAAT1 wt CDS-insert, the EAAT1 Δ3-CDS insert or the EAAT1 Δ9-CDS insert. Table 3.1 gives an overview of the primer pairs used and the expected product sizes if the for each type of insert.

The protocol used for the PCR-Colony-Screening is as follows:

1. Material of 10 single colonies grown on LB-Agar plates conatining 0.1 mg Ampicillin per 1 ml LB-Agar was put into 200 μl of ddH_2O,
2. This was boiled for 5 min to disrupt the cells and then centrifuged at 3000 g for 5 min to sediment cell debris.

3. 1 μl was taken and used as template in a standard PCR reaction.
4. The PCR-product was run on a 2% Agarose gel to identify batches containing inserts of the category 2 described above.
5. Material of the single colonies that the original batch consisted of was taken and put into 50 μl of ddH_2O and subjected to steps 2 to 4.

Single colonies that were identified to belong to category 2 were grown in 5 ml of LB-medium (0.1 mg Ampicillin per 1 ml LB-Medium) over night at 37°C, 150 rpm. Of each grown colony a glycerol stock was prepared as described in section 3.5. From 4 ml of each over night culture plasmids were isolated as described in 3.6.

3.11.2 Sequencing of Plasmid DNA

Plasmids isolated from the colonies that gave positive results in the PCR-Colony-Screen were sequenced to get a 100%-verification for the inserts being identical with either the EAAT1 wt-, the EAAT1 Δ3- or EAAT1 Δ9-CDS. The Applied Biosystems BDT v3.1 Sequncing kit was used to do the dye termination reaction which is based on the Sanger-dideoxy-method [73]. Each type of the chain-terminating dideoxynucletides is labeled with a different fluorescent dye for later detection. The protocol for the BDT-sequencing reaction was as follows: Between 100 ng and 200 ng of extracted plasmid DNA were mixed with 0.5 μl of BDT v3.1 reagent, 3.75 μl of sequencing buffer, 7 pmol of sequencing primer and adjusted to a volume of 15 μl with H_2O. The mixture was then subjected to the following program in the MJ Thermocycler:

1. 94°C for 5 min
2. 94°C for 30 sec
3. Annealing temperature of the used sequencing primer for 15 sec
4. 60°C for 4 min
5. Repetition of step 2 to 4 for 40 times
6. 10°C ∞

The sample was then subjected to EDTA/EtOH precipitation as described in section 3.7 and taken to the Australian Genetics Laboratory (AGL) through which the sequencing was done using an Hitachi 3130xl Genetic Analyzer with a 16 Capillary 50cm array and Performance Optimized Polymer 7 (POP 7) from Applied Biosystems.

3.12 SYBR® Green I Real-Time PCR for mRNA-Quantification

Quantitative real-time reverse transcription polymerase chain reaction (real-time RT-PCR) is the up to date method to assess gene expression levels with high sensitivity, specificity and reproducibility [74]. This standard PCR based technique has a dynamic range of 7-8 orders of magnitude and thereby offers more sensitivity than any other RNA quantification method developed so far [63]. SYBR® Green I real-time PCR was used as method in this project, using the more stable cDNA as template which was transcribed under standardized conditions (see section 3.9.2) from total RNA extracts of sampled cases and areas to ensure comparability. So to say, a two-step-two-tube real-time RT-PCR was done.

SYBR® Green I fluoresces when bound to the minor groove of double stranded DNA, product accumulation can thereby be measured on per cycle basis[75]. Absolute quantification was used in this project, using plasmid standards containing each of the EAAT1 variants to be quantified. A dilution series of the standard for each variant was created with a range of 7.5×10^5, 5×10^5, 5×10^4, 5×10^3 and 5×10^3 copies. Concentrations of each dilution were checked using UV spectrophotometry and copy number was calculated using the following formula:
Copy number of interest = mass of plasmid taken/mass of single plasmid molecule [76].
The ABI Prism® 7900 Sequence Detection System was used with 384 well plates. Each dilution of each standard was run in triplicates on each plate. C_t values (C_t=fractional threshold cycle number) of each standard dilution was plotted against the corresponding copy number. This allowed for a linear regression and calculation of a and b parameters of C_t values as function original copy number in form of:

$$C_t = a\times\text{copy number}+b$$

Given the parameters, this equation could then be used to calculate copy numbers of samples according to their C_t value.

The cDNA transcribed from total RNA-extracts of selected cases and areas was used as samples for quantification. All sample quantifications were done in duplicate. For each reaction 1 μl of cDNA (1:3 diluted) was placed into 9 μl reaction mixture containing 5 μl of SYBR® Green I PCR Master Mix and a final concentration of 300 nM of each primer. On each plate a no template control (NTC) was run as to check for possible contamination of reagents.
ROX was used as passive reference fluorescent agent already contained within the SYBR Green I PCR Master Mix. All real-time PCRs were performed using the following cycling protocol: initial incubation at 95°C for 10 min, followed by 40 cycles at 95°C for 15 sec and 62°C for 60 sec.

Thermal cycling was followed be a melting curve analysis, where fluorescence intensity is measured during temperature ramping from 60°C to 95°C. At 60°C all DNA is double stranded and fluorescence is highest whereas at 95°C all dsDNA is melted to ssDNA, the fluorescence intensity being the lowest.

A single peak at the melting temperature of the expected product indicates that no other unspecific product has been produced. More then one peak in the melting profile indicates the presence of more than product and therefore unspecific amplification *or* the presence of a product in which different parts melt at different temperatures due to for example high AT-content in some parts of the sequence. When more then one peak occurs in the melting curve analysis the real-time PCR-product should be run out on an agarose gel to examine whether there is only a single band i.e. one product or more bands indicating unspecific products.
Even if only one band shows up the gel, it is not yet certain that there is not another product of very low yield. Sequencing of the whole product is then a way to assess whether only one sequence i.e. one product is detected or whether sequence overlapping peaks occur which would then definitively prove the presence of an unspecific product.

Chapter 4

Results

4.1 Detection of EAAT1 wt, △3- and △9-Variants in Pooled cDNA of Control Cases

EAAT1 CDS FP and EAAT1 CDS RP primers were used in an Elongase® Enzyme Mix PCR with pooled cDNA (transcribed from total RNA extracts) from control cases as template as to amplify the whole CDS of any EAAT1 variant present. PCR conditions were optimized by running a temperature gradient PCR (cycling conditions: 94°C for 10 min followed by 40 cycles at 94°C for 30 s, different annealing temperatures for 30 s and 68°C for 90 sec, followed by a final extension at 68°C for 10 min). PCR products were subjected to 3.5% PAGE analyses. Thereby 55°C as annealing temperature was found to be optimal. Figure 4.1 shows that at optimal conditions only one band of the size of about 1630 bp is detectable. This band therefore represents the EAAT1 wt CDS amplicon with a size of 1628 bp.

No bands of lower size, i.e. variants of EAAT1 were detectable which is probably due to both low yield (it is expectable the variants occur in a much lower copy number than the wt) and poor resolution of the polyacrylamide gel.

To solve the resolution issue, primer pairs of EAAT1 exon 2a FP/EAAT1 exon 4 RP and EAAT1 exon 8 FP/EAAT1 exon 10 RP were used in a standard PCR applying the same conditions as above.

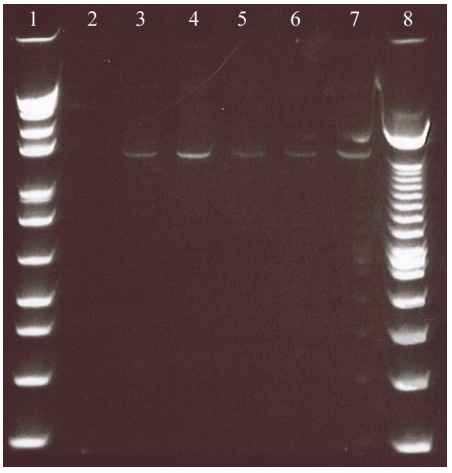

Figure 4.1: Temperature gradient PCR with EAAT1 CDS FP and RP

A 3.5% polyacrylamide gel was loaded with 1) 1 kb ladder, 2) NTC and each 5μl PCR-products of reactions run at different annealing temperatures of 3) 53°C, 4) 55°C, 5) 57°C, 6) 59°C and 7) 61°C. Lane 8) was loaded with 100 bp ladder.
At 55°C the product yield is the highest. Rising of the annealing temperature results in production of unspecific products as seen in lane 6) and 7) where the band of the right product size is accompanied by another, larger product.

Figure 4.2 shows that the EAAT1 Δ9-variant was detected. The EAAT1Δ3-variant was not detected which could still be due to low yield. As shown in section 4.2, the EAAT1Δ3-variant was detected later on during PCR colony screening using the primer pairs used cited above.

4.2 Cloning of EAAT1 variants

For the ligation reaction of the Elongase® Enzyme Mix PCR-product into the pGEM®-T Easy Vector, a 5:1 insert to vector ratio was found to be optimal (data not shown). Scanning the colonies for the cloned inserts using the classical approach proved to be very time and cost consuming.
To achieve higher throughput, PCR-colony screening was applied. The EAAT1 exon 2a FP/EAAT1 exon 4 RP and EAAT1 exon 8 FP/EAAT1 exon 10 RP primer pairs (see table 3.1 were used to screen 100 colonies for all variants of EAAT1. Most of the colonies contained the EAAT1 wt inserts, however two colonies contained the Δ3- and one colony contained the Δ9-variant (data not shown).
The found clones of the EAAT1 wt, EAAT1 Δ3- and Δ9-variants were sequence verified.

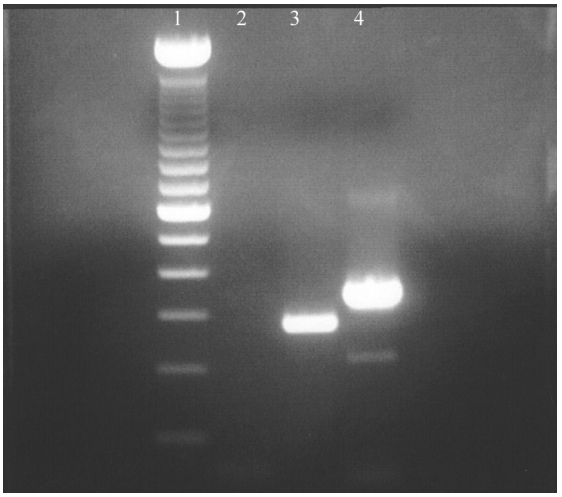

Figure 4.2: Amplification of Parts of the EAAT1 CDS for Detection of Splice Variants

A 2% agarose gel was loaded with 1) 100 bp ladder, 2) NTC and each 25μl PCR-products of reactions with different primer pairs being 3) EAAT1 exon 2a FP/EAAT1 exon 4 RP and 4) EAAT1 exon 8 FP/EAAT1 exon 10 RP using pooled cDNA from control cases as template.
Only one band of about 280 bp is detectable in lane 3). According to its size this band represents the expected amplification product of the wt. There is no smaller product, indicating that there is no or only very little EAAT1 Δ3 variant in the template.
Two bands are present in lane 4). The larger band of about 360 bp represents the expected amplification product of the wt whereas the smaller band of about 220 bp represents the expected amplification product of the Δ9-variant. See table 3.1 for expected product sizes.

4.3 Optimization of Primer Purification Using Denaturing PAGE

To ensure complete specificity, some of the primers used in real-time PCR were subjected to PAGE purification as described in 3.4.2. Using 0.75 mm thick polyacrylamide gels resulted in an odd bubble-effect when more than 1μg of primer was loaded per well (an amount totally inappropriate for time/cost-effective purification) as may be seen in figure 4.3.

First assuming this was due to a production error of the supplier, SIGMA Genosys was contacted and consulted. The company had seen this "bubble-effect" before and it was said that it had merely to do with the thickness of the gel —at SIGMA Genosys it is common to use 4 mm thick gels for primer purification.

When the thickness of the gels used in this project was changed to 2.25 mm, no bubble-effect was detected and up to 10 μg of primer could be loaded per well with good seperation results as shown in figure 4.3.

On average about 80% of the primer loaded onto a gel could be recovered with the freeze/thaw-method described in section 3.4.2.

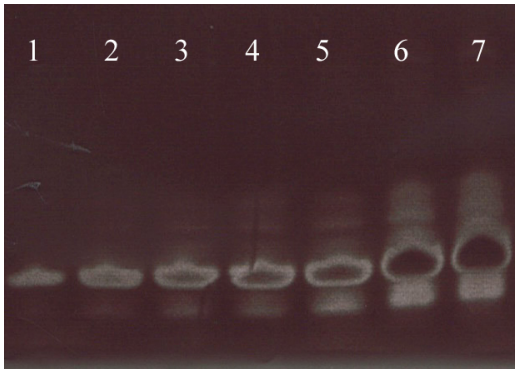

(a) Primer purification using a 0.25 mm thick polyacrylamide gel

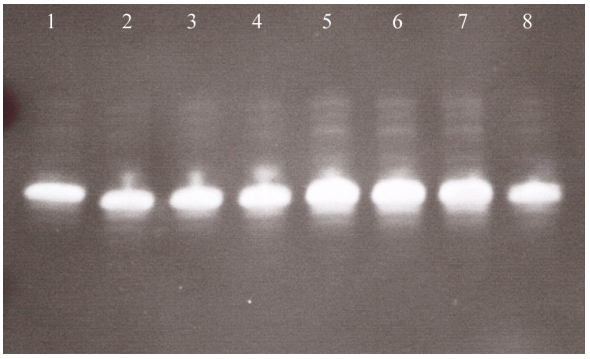

(b) Primer purification using a 2.25 mm thick polyacrylamide gel

Figure 4.3: Primer Purification Using Denaturing PAGE

20% polyacrylamide, 7 M urea gels were used. Gel a) was loaded with different amounts of the same primer ranging from 0.5 μg in lane 1) to 10 μg in lane 7). The bubble effect occured when more then 1 μg were loaded.
Gel b) was loaded with 10 μg of the same primer in each lane. No bubble effect occurs.
Smears under the main band indicate the presence of degraded primers, bands above indicate the presence of primers with residues of the protection groups used during synthesis.

A possible explanation for the bubble-effect may be the overloading of the polyacrylamide matrix with ssDNA, leading to a locally very high resistance and dropping of voltage, resulting in the "flowing around" of the electrical and fluidal current.

4.4 Optimization of the EAAT1 Variants Quantification Using Real-Time PCR

It was already known, that when quantifying exon skipping splice variants, primer specificity is a major problem [63] and as mentioned in section 3.8.3 the possibilities of primer design are very restricted. Before doing the actual quantification of the EAAT1 variants in the samples, all primer pairs designed for that purpose were therefore tested in standard PCR reactions with real-time PCR cycling conditions with the standards of each variant to assess their specificity.

Figure 4.4 shows the result of the specificity assessment using the EAAT1 exon 2b FP/EAAT1 exon 4 RP, EAAT1 exon 3skip4ovlap FP/EAAT1 exon 3 skip RP, EAAT1 exon 8 FP/EAAT1 exon 8/9 RP and EAAT1 exon 8 FP/EAAT1 exon 9skip3ovlap RP primer pairs on all three standards.
The EAAT1 wt amplifying primer pairs did not show cross amplification with the standards for the

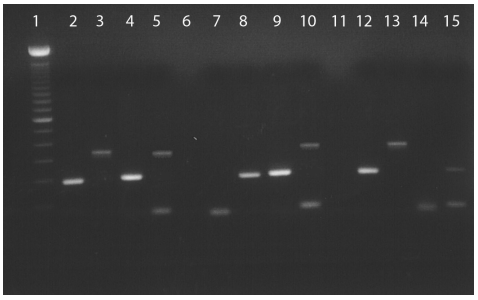

Figure 4.4: Specificity Assessment of Primers

Loading scheme for this 2% Agarose gel was as follows: Lanes 2-5: EAAT1 wt-standard as template (1Mio cop); Lanes 7-10: EAAT1 Δ3 standard as template (1Mio cop); Lanes 12-15: EAAT1 Δ3 standard as template (1 Mio cop). Different primer pairs were used:
Lanes 2; 7; 12: EAAT1 exon 2b FP/EAAT1 exon 4 RP
Lanes 3; 8; 13: EAAT1 exon 3skip4ovlap FP/EAAT1 exon 3 skip RP
Lanes 4; 9; 14: EAAT1 exon 8 FP/EAAT1 exon 8/9 RP
Lanes 5; 10; 15: EAAT1 exon 8 FP/EAAT1 exon 9skip3ovlap RP primer pairs
No cross amplification was detectable for primer pairs designed to amplifying EAAT1 wt sequence parts. The bands in lanes 3, 5, 10 and 13 of about 330 bp in size show that the primer pairs that amplify the exon skipping variants also amplify parts of the wt sequence.

splice variants but amplified only their target sequence.

Yet the primer pairs amplifying either one of the variants did not only amplify their target sequence but also EAAT1 wt.

noindent PCR conditions were optimized by running temperature and primer concentration gradients and PAGE purifying the exon-exon-boundary spanning primers to exclude possible cross-amplification caused by degraded primer. Neither of those approaches showed any significant improvement of specificity of the primers (data not shown). This led to the assumption that the primer design must be sub optimal and a closer look at the sequences of the exon-exon-boundaries revealed that both EAAT1 exon 3skip4ovlap FP and EAAT1 exon 9skip3ovlap RP showed complementarity at their 3'-end not only with their target sequence of the corresponding variant but also partly with the wt sequence. Figure 4.5 shows the exon-exon boundaries of the EAAT1 wt and the two splice variants in alignment with the different primers designed to specifically amplify the EAAT1Δ3 and EAAT1Δ9 variants, respectively.

Looking at the alignment it is revealed that at their 3'-end, the 3skip4ovlap FP is complementary to the EAAT1 wt sequence at the beginning of exon 3 at two positions and that the 9skip3ovlap RP is complementary to one position the EAAT1 wt at the beginning of exon 9. It was then concluded that both primers were not usable as they had too much in common with the corresponding parts of the wt

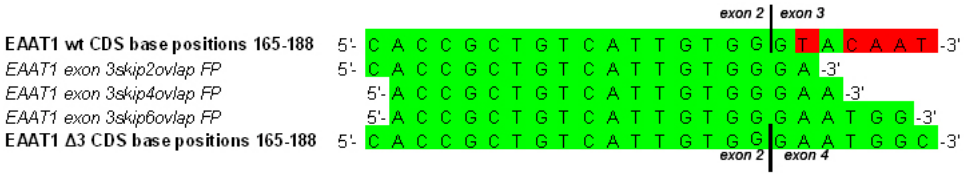

(a) Alignment of primers designed to specifically amplify EAAT1 Δ3 with their target sequence and the EAAT1 wt sequence

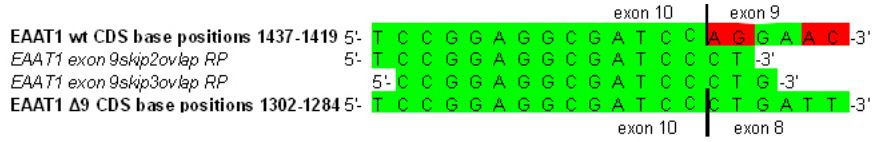

(b) Alignment of primers designed to specifically amplify EAAT1 Δ9 with their target sequence and the EAAT1 wt sequence

Figure 4.5: Alignment of Different Primers with their Target Sequence and Sequence Parts of EAAT1 wt Causing Possible Cross-Amplification

Target sequences for the primers a aligned at the bottom, sequence parts of EAAT1 wt causing possible cross-amplification are aligned at the top in a) and b), respectively.
Sequence parts shaded green are identical whereas redly shaded parts are different from the rest.

sequence.

Subsequently the EAAT1 exon 3skip2ovlap FP was substituted for the 3skip4ovlap FP and assessed for possible cross-amplification of the EAAT1 wt. Cross-amplification occured and could not be solved by optimizing reaction conditions like annealing temperature and primer concentration (data not shown).

This is thought to be due to the fact that only the very last base at the 3'-end of the primer is actually different from the corresponding wt sequence (Figure 4.5. As mentionend earlier, the polymerase is most probably able to override that one mismatching base when the primer bind to the wt and therefore amplification is possible.

The EAAT1 exon 3skip6ovlap FP and the EAAT1 exon 9skip2ovlap RP were subjected to testing for cross-amplification of the EAAT1 wt. After initial problems, changing the primer concentration to a final 90 nM in case of EAAT1 exon 3skip6ovlap FP and to 210 nM in case of EAAT1 exon 9skip2ovlap RP showed amplification results with no cross-amplification as may be seen in figure 4.6.

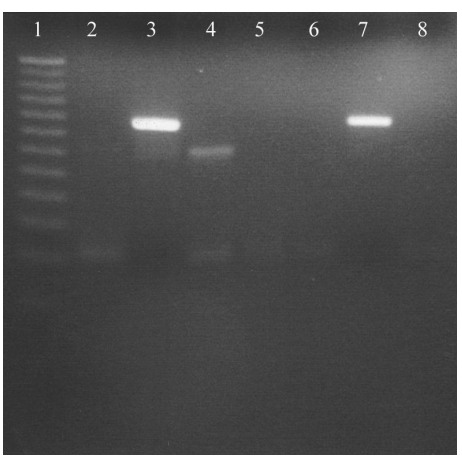

(a) Usage of different concentrations of EAAT1 exon 3skip6ovlap FP on with plasmid standards of all EAAT1 variants (wt, Δ3 and Δ9)

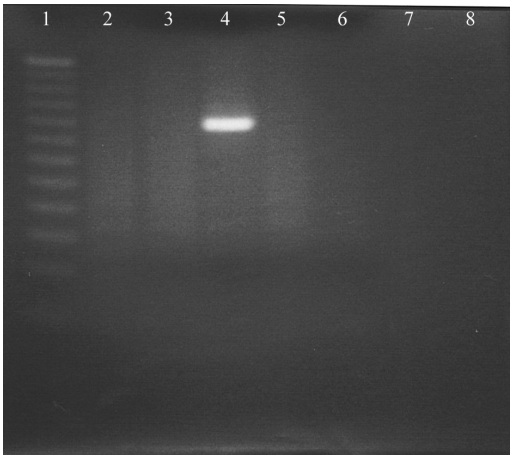

(b) Usage of different concentrations of EAAT1 exon EAAT1 exon 9skip2ovlap RP on with plasmid standards of all EAAT1 variants (wt, Δ3 and Δ9)

Figure 4.6: Assessment of EAAT1 wt Cross Amplification with Different Primers

Gel a) was loaded with 25 bp ladder in lane 1. Lanes 2 to 4 were loaded with PCR products of different templates using the EAAT1 exon 3skip6ovlap FP/EAAT1 exon 3 skip RP primer pair in a final concentration of 210 nM for each primer. Templates were 1 Mio copies of the plasmid standards: 2) EAAT1 wt, 3) EAAT1 Δ3 and 4) EAAT1 Δ9. Lane 5 was loaded with a NTC. Lanes 6 to 8 were loaded with the same template order as in lanes 2 to 4 but a final concentration of 90nM of each primer was used.
As may be seen, not crossamplification of the wt sequence in the exon 2 to 4 area occures, when primer concentration is dropped to 90 nM, only the target sequence was amplified.
Gel b) was loaded with 25 bp ladder in lane 1. Lanes 2 to 4 were loaded with PCR products of different templates using the EAAT1 exon 8 FP/EAAT1 9skip2ovlap RP primer pair in a final concentration of 210 nM for each primer. Templates were 1 Mio copies of the plasmid standards: 2) EAAT1 wt, 3) EAAT1 Δ3 and 4) EAAT1 Δ9. Lane 5 was loaded with a NTC. Lanes 6 to 8 were not loaded.
No crossamplification of the wt sequence in the exon 8 to 10 area is detectable, only the target sequence was amplified.

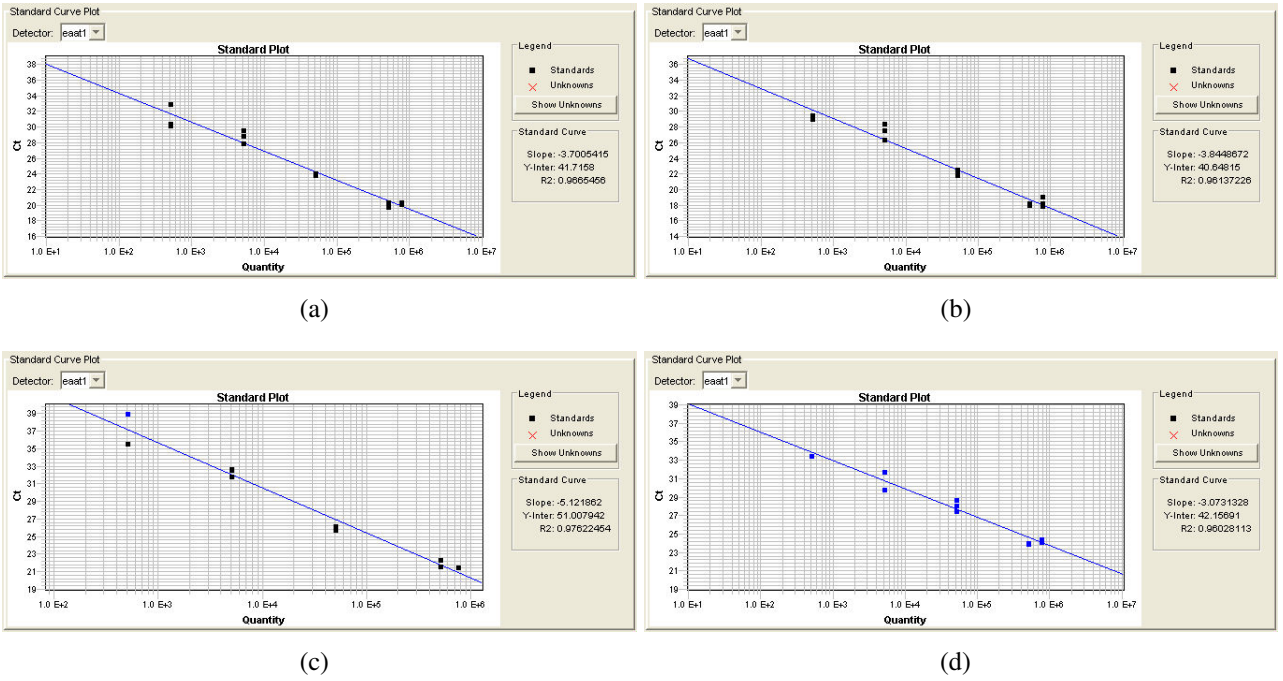

Figure 4.7: Linear Regression for Standards of Different EAAT Variants

Linear regressions for the EAAT1 wt standard amplified in the a) exon 2 to 4 area and b) the exon 8 to 9 area are shown. In c) and d) linear regressions are shown for the amplification of the EAAT1 Δ3 standard and the EAAT1 Δ9 standard, respectively.
C_t-values are plotted against the total copy number of each dilution step, ranging from 500 to 7.5×10^5cop.

4.5 Validation of EAAT1 wt, Δ3 and Δ9 Plasmid Standards

The dilution series of each plasmid standard was run in triplicate in each real-time PCR. Linear regression was analysis of the data for the standards was carried out as described in section 3.12. R^2 values were used to assess the quality of the standard dilutions and were in a range between R^2=0.96 and 0.97.

Standards were run several times in real-time PCRs, showing to be invariant. It is therefore assumable that there is none or only little degradation of the plasmid DNA. Figure 4.7 shows the linear regressions of the standards for each run plate.

4.6 Melting Curve Analysis

As mentioned in section 3.12 a melting curve analysis was run after the cycling program in each real-time PCR. Melting curves of standards and samples were checked after each real-time PCR and in

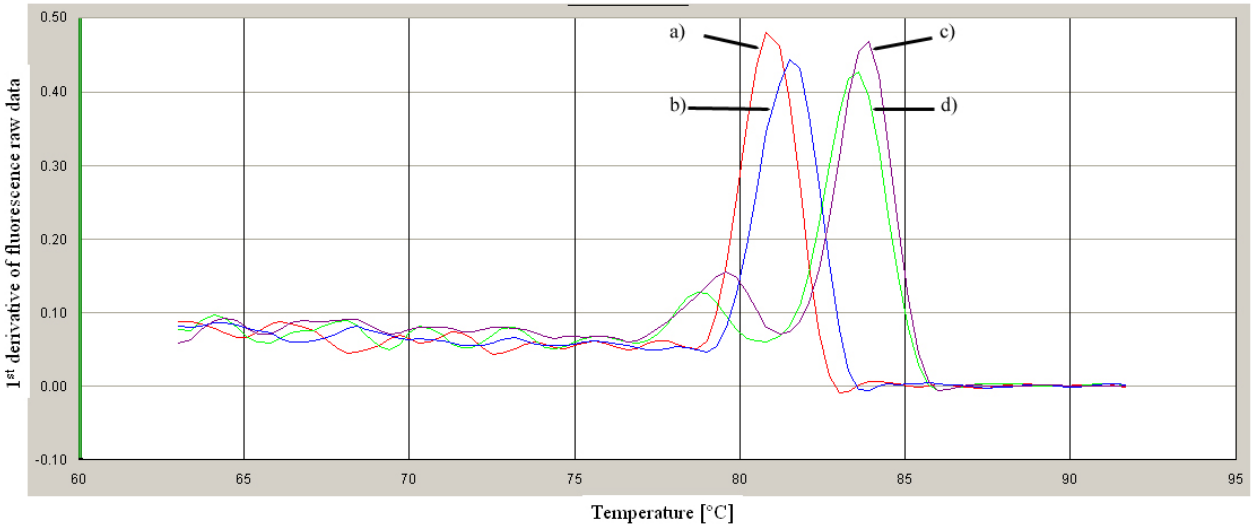

Figure 4.8: Representative Melting Curves of Different Products Quantified

Melting curves for different real-time PCR products using a) the EAAT1 exon 2b FP/EAAT1 exon 4 RP, b) the EAAT1 exon 3skip6ovlap FP/EAAT1 exon 3 skip RP, c) the EAAT1 exon 8 FP/EAAT1 exon 8/9 RP and d) the EAAT1 exon 8 FP/EAAT1 exon 9skip2ovlap RP primer pairs are shown. Only one product peak is seen in a) and b) whereas two peaks are detected in c) and d). Possible reasons for the latter are given below.

figure 4.8 representative melting curves for each of the four different products are shown.

The products of the real-time PCRs using the EAAT1 exon 2b FP/EAAT1 exon 4 RP and EAAT1 exon 3skip6ovlap FP/EAAT1 exon 3 skip RP primer pairs show feature only one clear peak, proving that only one product is present and no cross-amplification took place.

In contrast, the melting curves of the real-time PCR products using the EAAT1 exon 8 FP/EAAT1 exon 8/9 RP and EAAT1 exon 8 FP/EAAT1 exon 9skip2ovlap RP primer pairs show two peak which occurred in all samples and standards alike.

Cross-amplification of another variant as cause for the small peak can be excluded because its melting temperature is much lower than the predicted melting temperature of a possible cross-amplification product which would be 135 bp longer (the length of exon 9). Moreover the smaller peak occurred with the plasmid standard as well, where cross-amplification of another variant is impossible.

To totally exclude possible unspecific amplification, the products of the real-time PCR were analysed on a 2% agarose gel. As shown in figure 4.9 only one band is detectable, indicating the presence of only one product. Additionally the real-time PCR products were sequenced: only one sequence

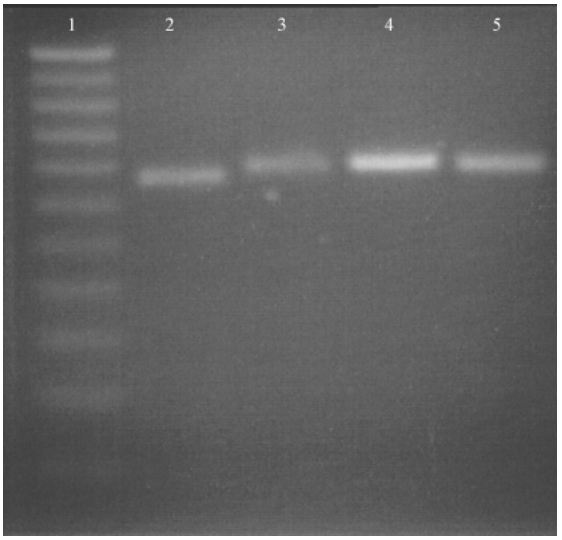

Figure 4.9: Products of a real-time PCR analysed on 2% Agarose

Lane 1) was loaded with 25 bp ladder. Different real-time PCR products of reactions with 2) the EAAT1 exon 2b FP/EAAT1 exon 4 RP, 3) the EAAT1 exon 3skip6ovlap FP/EAAT1 exon 3 skip RP, 4) the EAAT1 exon 8 FP/EAAT1 exon 8/9 RP and 5) the EAAT1 exon 8 FP/EAAT1 exon 9skip2ovlap RP primer pair were loaded. The products in lanes 4) and 5) had shown two peaks in the melting curve analysis but only one product band is detectable, indicating the presence of just one product.

was detectable, proving that only specific amplification occurs.

A possible reason for the first little peak is the higher AT content in some areas (see figure 4.10) of the produced amplicons which therefore melt at lower temperatures whereas the rest of the amplicon melts at higher temperatures. This two-step melting process would then result in two peaks in the melting curve plot.

4.7 Assessment of the Reproducibility of the Used Quantification Method

For the assessment of the method the raw data of the measurements was used since mathematical transformation of data as the $\log_2$ transformation used in the sections below would artificially change errors inherent to the experiment. Stated means are therefore different to the ones calculated with the $\log_2$ transformed data.

Two measures were calculated to determine the accuracy and reproducibility of the method devel-

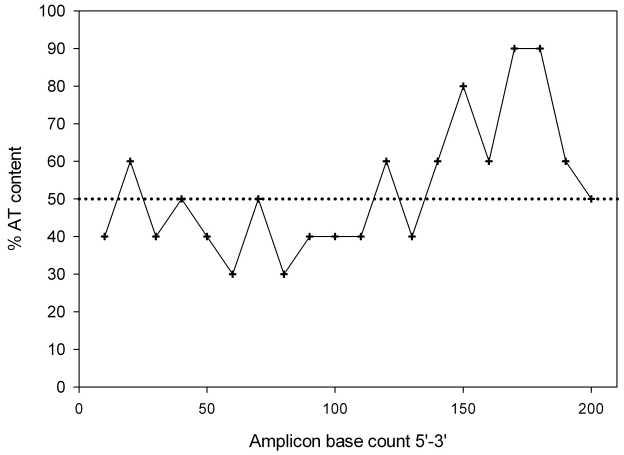

(a) AT content plot of the amplicon produced using the EAAT1 exon 8 FP/EAAT1 exon 8/9 RP primer pair

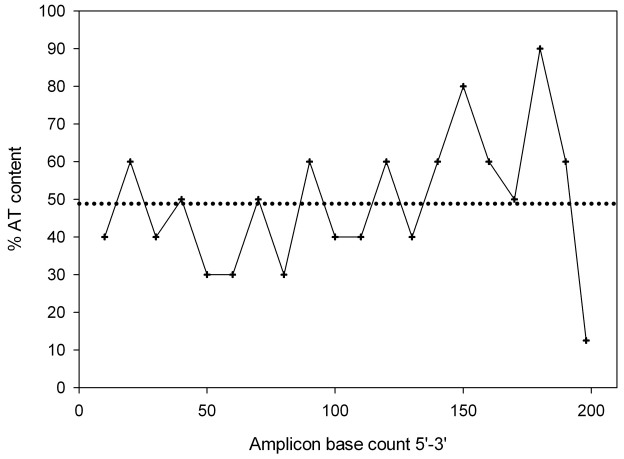

(b) AT content plot of the amplicon produced using the EAAT1 exon 8 FP/EAAT1 exon 9skip2ovlap RP primer pair

Figure 4.10: AT Content Plots of Different Amplicons

As may be seen in both AT content plots, in either of the amplicons the AT content is higher at their 3'-end than the mean AT content of the whole amplicon which is marked by the dotted line. Those ends are thought to melt at lower temperatures than the rest of the amplicon, therefore leading to a two-peak melting curve.

oped for absolute quantification of the EAAT1 variants (wt, $\Delta 3$ and $\Delta 9$):

- The over all mean of standard deviations of the two measures taken per sample was calculated to be 11.07%.
- The mean of the EAAT1 wt copy number over all cases and areas combined was determined to be $5{,}45 \times 10^5$ cop per μg total RNA extract for the wt amplified in the exon 3-4 area and 6.77×10^5 cop per μg total RNA extract for the wt amplified in the exon 8-9 area. This resembles a difference of 24% between the two means, which theoretically should be 0%. This didn't have any effect on the comparative analysis in section 4.8 as data sets were only compared within themselves and not with each other: The percentage of EAAT1 wt expression in AD cases compared to controls was calculated. It came out to be 16% of EAAT1 wt when working with the data set for the EAAT1 wt detection in the exon 3-4 area compared to 18% when working with the data set for the EAAT1 wt detection in the exon 8-9 area. Statistics done with either of the data sets did not show any significant difference in their outcomes. When refering to EAAT1 wt results in the sections below, the data set for the EAAT1 wt detection in the exon 3-4 area was bases for analysis and plotting of data.

4.8 Comparative Analysis of the Copy Numbers of all EAAT1 Variants

The data sets for each EAAT1 variant were checked for normal distribution, as the used statistical method (independent, two tailed t-test) is based on the assumption that the inputted data is normally distributed.

Normal probability plots and Shapiro-Wilk tests were done for all data sets. Figure 4.11 states that the data shows a skewed distribution, i.e. it is not normally distributed ($P<0.05$). To minimize effects on further statistical analysis, all data sets were $\log_2$ transformed and again subjected to Shapiro-Wilk tests accompanied by normal probability plots. Figure 4.11 shows that the data is still skewed but closer to being normally distributed than before the $\log_2$ transformation. All further statistical analysis was therefore done with the transformed data. The calculated means presented below were all calculated by re-transforming the means calculated with the $\log_2$ transformed data to their original scale of measurement.

To assess the integrity of RNA quality and to rule out the possibility that a difference in total copy

numbers of the EAAT1 transcripts is due to different post mortem delays (PMD), total copy numbers were plotted against PMD and subjected to regression analysis. No correlation was found ($P>0.5$; data not shown).

Comparative Analysis of Total Copy Numbers of all Variants in all Case Groups

For all variants of EAAT1 a reduction of transcription in AD cases compared to controls is visible. This applies for all areas examined in a similar pattern as may be seen in figures 4.12, 4.13 and 4.14. In the posterior motor and occipital pole area of AD cases the reduction of the mean EAAT1 $\Delta 9$ transcription was not as big as in the inferior frontal and inferior temporal areas, yet still significantly lower than in the same areas in controls (see section 4.9 for further analysis of this phenomenon).

In regard to the total copy number one can therefore state that generally no significantly different transcription patterns were detected in between different areas. for either of the quantified variants.

Compared to control cases the average transcription of EAAT1 wt drops 84%, the EAAT1 $\Delta 3$ transcription 95% and the EAAT1 $\Delta 9$ transcription 80% in AD cases. Figure 4.15 shows the transcription pattern of the EAAT1 variants when all areas are combined, the graphs feature the same pattern that was visible for the single area plots in figures 4.12, 4.13 and 4.14. The data sets were subjected to two-tailed independent t-tests, showing that the transcription of all EAAT1 variants is significantly lower in AD cases than in control cases ($P<0.0001$ for all EAAT1 variants).

Comparative Analysis of Total Copy Numbers in Males and Females

Mean copy numbers of all EAAT1 variants in control and AD case groups where t-tested for gender differences. None was found for neither the EAAT1 wt copy number (see figure 4.16) nor the copy number of the variants (data not shown).

4.9 Comparative Analysis of the Percentage of Splice Variants of EAAT1 wt

When combining all cases the mean proportion of EAAT1 $\Delta 3$ was found to be 0.15% of EAAT1 wt whereas the EAAT1 $\Delta 9$ proportion was found to be 26.6% of EAAT1 wt. The results are plotted in figure 4.17, the large 95% confidence intervals already suggest that there are vast differences in transcription of the EAAT1 variants between case groups as shown above.

Comparative, Area-Based Analysis of the Percentage of Splice Variants of EAAT1 wt

For the percentage of EAAT1 $\Delta 3$ of EAAT1 wt no significant differences between controls and AD cases were found in any of the examined areas (data not shown).

For the percentage of EAAT1 $\Delta 9$ of EAAT1 wt no significant differences between controls and AD cases were found in inferior temporal and inferior frontal areas (data not shown). Yet, in posterior motor and occipital pole areas of AD cases the percentage of EAAT1 $\Delta 9$ of EAAT1 wt is significantly higher ($P<0.01$) than in controls (see figure 4.18).

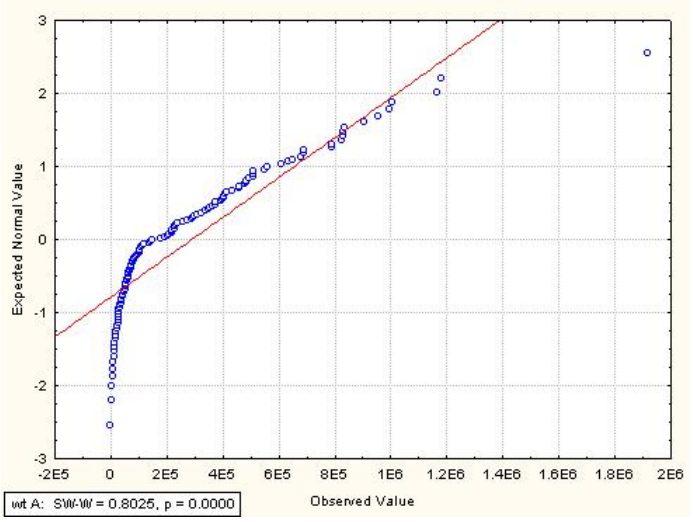

(a)

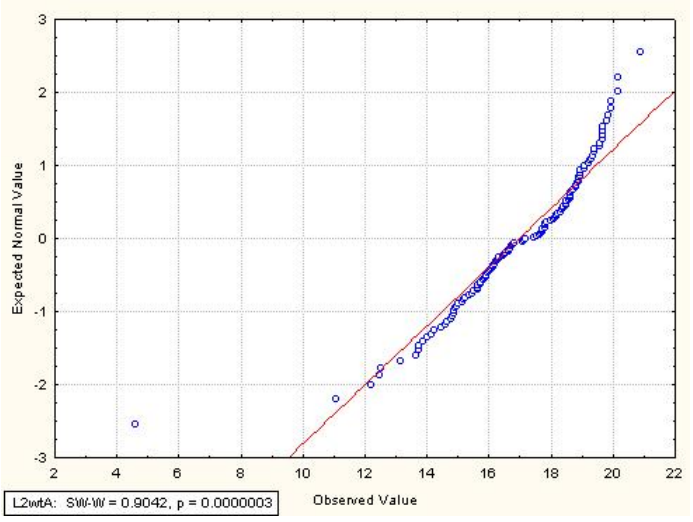

(b)

Figure 4.11: Normal probability plots of raw and transformed EAAT1 wt data sets

Shown are normal probability plots of a) the raw data of the EAAT1 wt total copy numbers and b) the same data set $\log_2$ transformed. It is clearly visible that the transformation results in a closer approximation of the data to normal distribution. The red diagonal shows the expected data-distribution based on the assumtion that it is normal. P-values are given stating that when P>0.05, data is normally distributed whereas when P<0.05, data is not normally distributed.

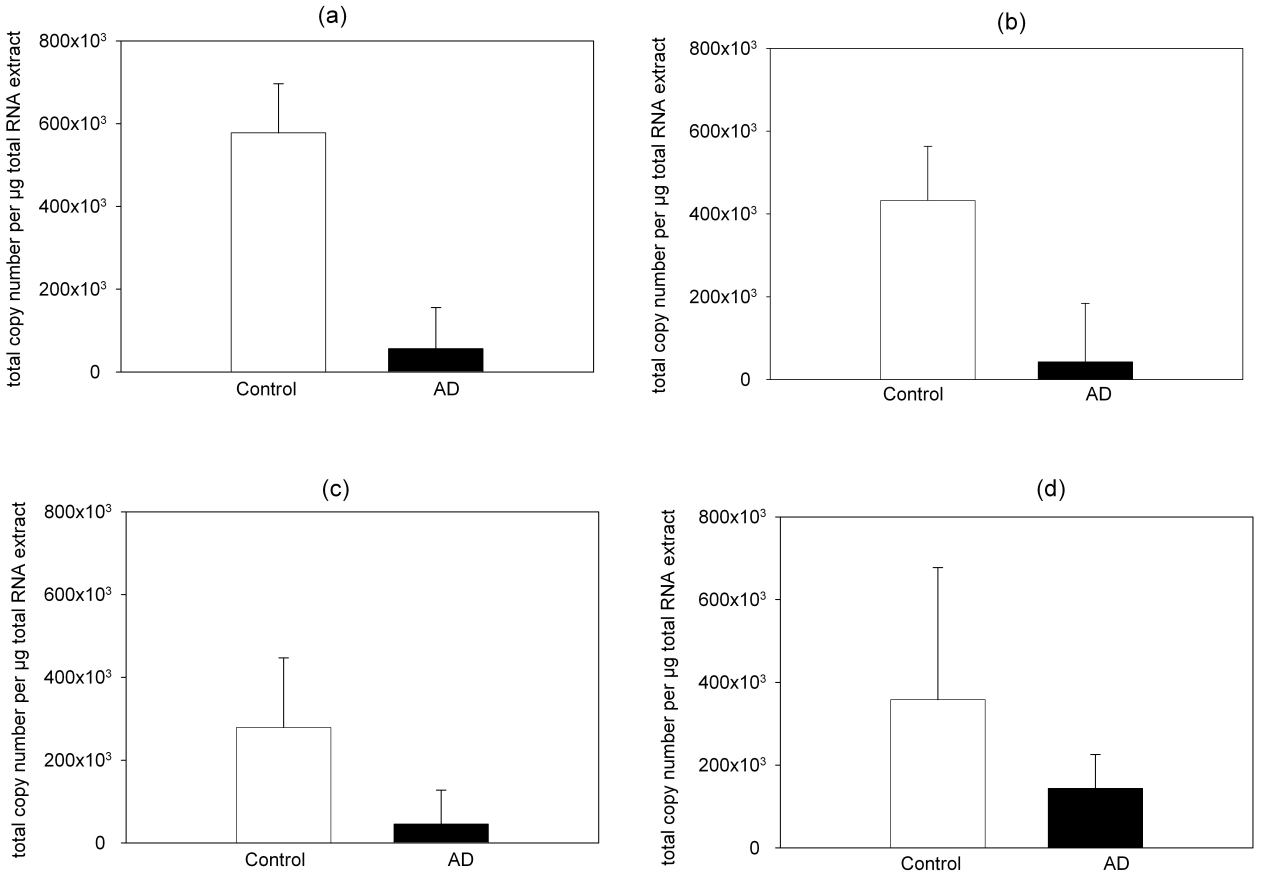

Figure 4.12: Transcription pattern of EAAT1 wt in different areas

Shown are the transcription patterns of EAAT1 wt comparing controls and AD cases in a) inferior temporal, b) posterior motor, c) occipital pole and d) inferior frontal areas.
Error bars denote 95% confidence intervals, as seen they are large in some cases which is caused by the data not being normally distributed which itself is partly due to the low number of cases examined.

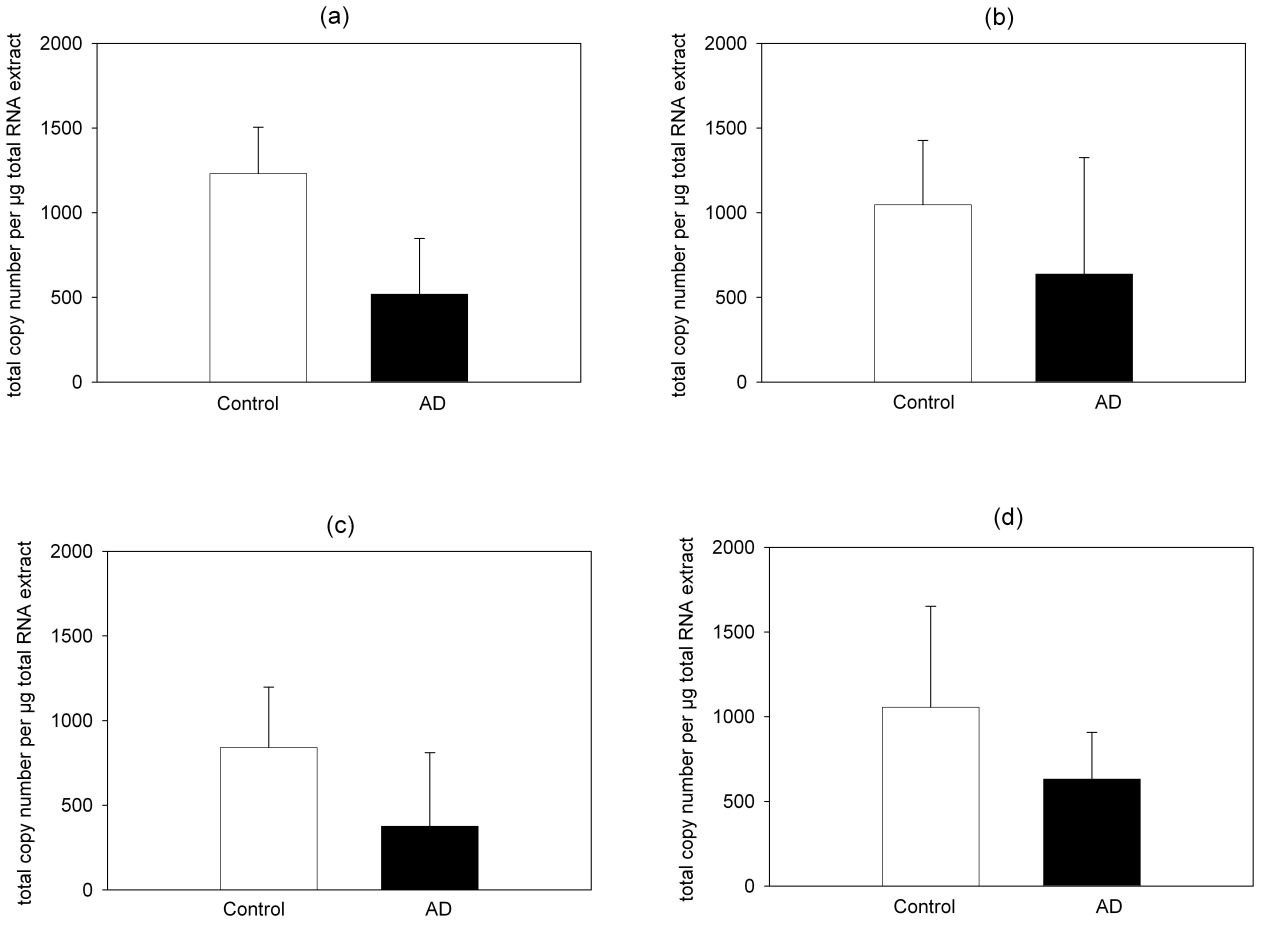

Figure 4.13: Transcription pattern of EAAT1 $\Delta 3$ in different areas

Shown are the transcription patterns of EAAT1 $\Delta 3$ comparing controls and AD cases in a) inferior temporal, b) posterior motor, c) occipital pole and d) inferior frontal areas.
Error bars denote 95% confidence intervals, as seen they are large in some cases which is caused by the data not being normally distributed which itself is partly due to the low number of cases examined.

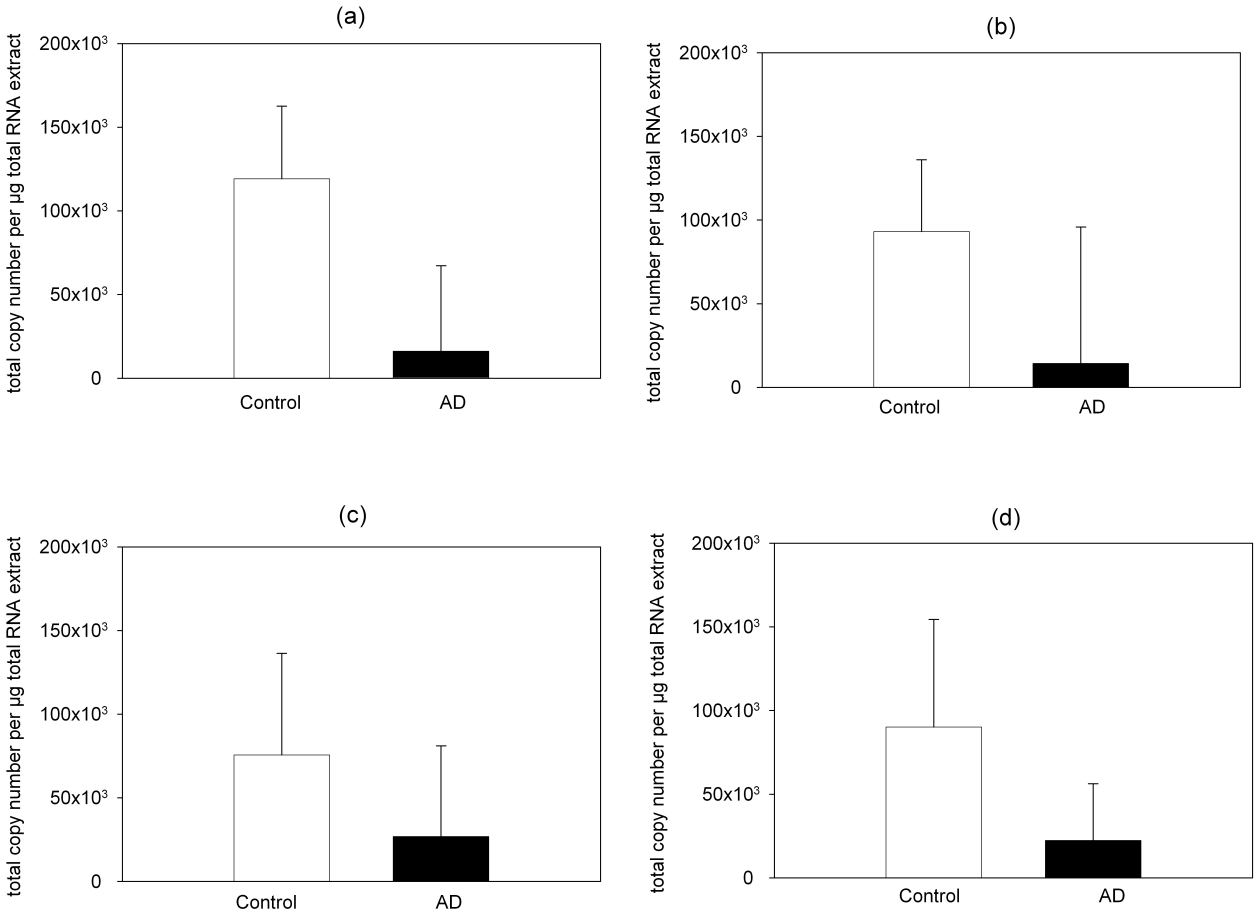

Figure 4.14: Transcription pattern of EAAT1 $\Delta 9$ in different areas

Shown are the transcription patterns of EAAT1 $\Delta 9$ comparing controls and AD cases in a) inferior temporal, b) posterior motor, c) occipital pole and d) inferior frontal areas.
Error bars denote 95% confidence intervals, as seen they are large in some cases which is caused by the data not being normally distributed which itself is partly due to the low number of cases examined.

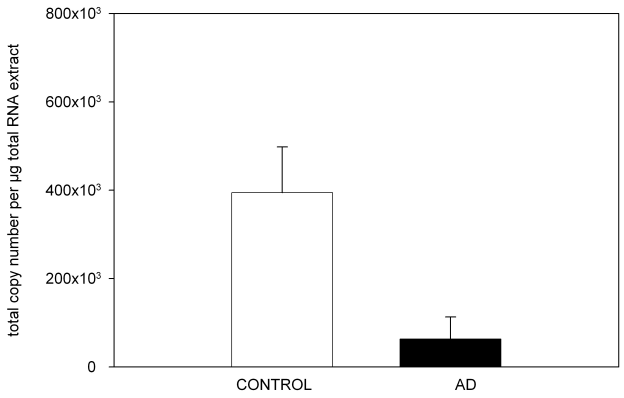

(a)

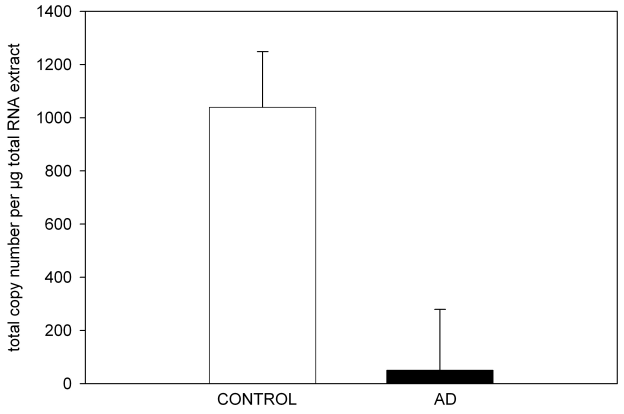

(b)

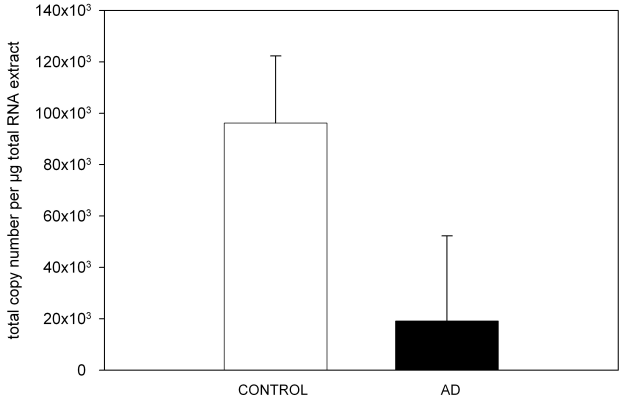

(c)

Figure 4.15: Transcription pattern of all EAAT1 variants, all areas are combined.

Shown are the transcription of patterns of the EAAT1 variants a) wt, b) $\Delta 3$ and c) $\Delta 9$, comparind controls to AD cases. For each variant the transcription is significantly lower ($P<0.0001$) in AD cases than in controls.
Error bars denote 95% confidence intervals.

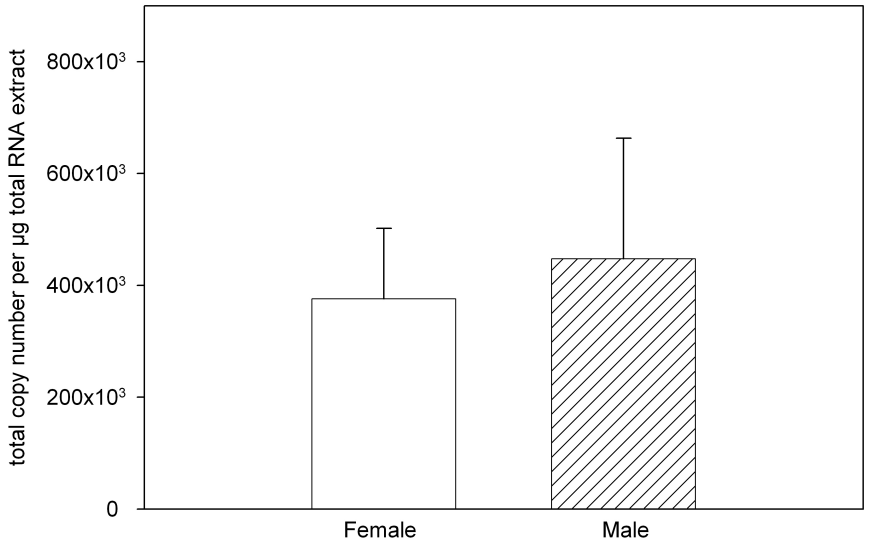

Figure 4.16: Mean EAAT1 wt copy number in male and female controls

The mean EAAT1 wt copy number in male and female controls is not significantly different (P=0.6). Error bars denote 95% confidence intervals.

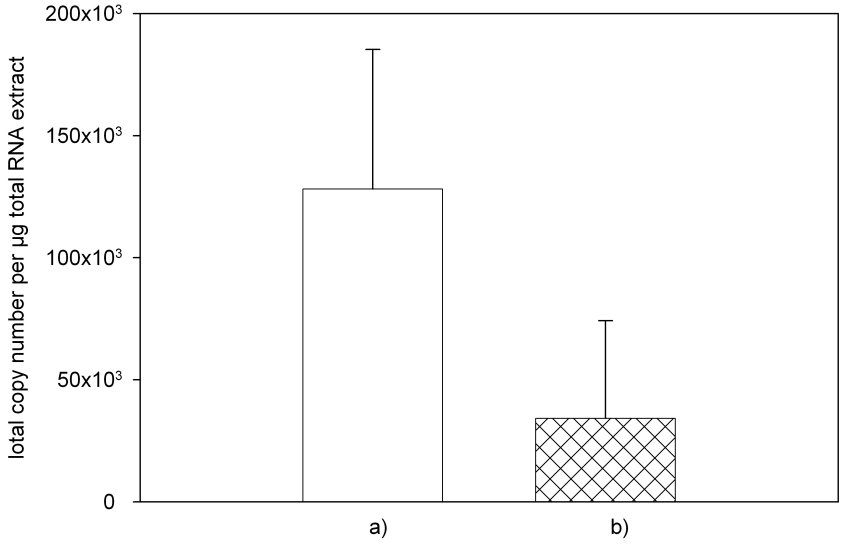

Figure 4.17: Comparison of the transcription of EAAT1 variants, all cases and areas combined

The graph shows that b) the EAAT1 $\Delta 9$ mean copy number is only about a quarter of a) the EAAT1 wt mean copy number. The EAAT1 $\Delta 3$ mean copy number is 137 copies per μg total RNA extract. It so low that it is out of scale and was therefore not plotted. Error bars denote 95% confidence intervals.

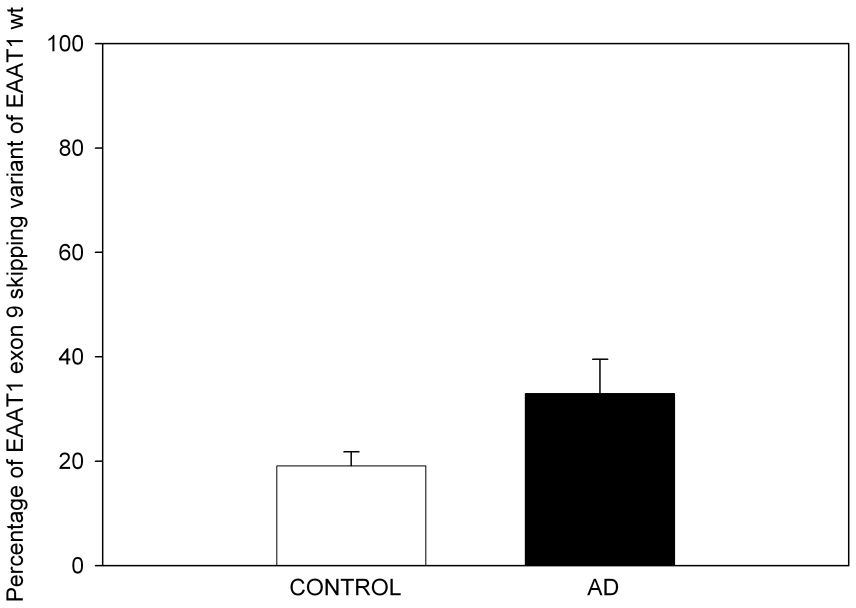

Figure 4.18: Percentage of EAAT1 $\Delta 9$ of EAAT1 wt, posterior motor and occipital pole areas combined

Percentage of EAAT1 $\Delta 9$ transcription of EAAT1 wt transcription is significantly higher in posterior motor and occipital pole areas of AD cases ($P<0.01$) compared to controls. Error bars denote 95% confidence intervals.

Chapter 5

Discussion and Conclusions

5.1 Method of Choice: SYBR® Green Real-Time PCR mRNA Quantification of Splice Variants

Primer Design of Exon-Exon-Boundary Spanning Primers

The experiences made in this project suggest that the length of the overlapping 3'-end of the primer is a rather secondary issue as long as it is at least two bases long which then must not be complementary with any other target that is to be quantified within the experiment. When constructing primers with a longer 3'-end it is crucial to design them in a way that the majority of overlapping bases are not complementary with any other target than the intended one—as shown in this project, it does not matter if only *some* bases of the overlapping 3'-end are complementary with other targets.

It was moreover shown that DST-purification of commercially produced primers features enough purity for real-time PCR, so to say the population of degraded primer is very small. It is therefore not an imperative to get the much more expensive PAGE-purified primers for projects such as this one. If there is any doubt about the grade of degradation a MS can help to assess that issue. If it then indeed proves to be a problem, the stated method of PAGE-purification in section 3.4.2 offers a quick and cheap method to purify primers.

General Design and Reproducibility

Being less sensitive to environmental contaminations such as RNases and moreover their feature of mimicking closely the unknown cDNA sample, plasmid standards with the full length sequence of the target cDNA were favored in recent publications [63, 77] as stable standards allowing for a high degree of reproducibility .

This was confirmed in this project where plasmid standards showed those very characteristics. Even though their accuracy is at least impaired through possible pipetting errors when doing the dilution series accompanied by errors of the concentration-measurements with UV-spectrophotometry. These errors are estimated to be very small, the source of the greatest error is the real-time PCR reaction itself. The exponential nature of PCR means that the slightest differences in standard and reagent concentrations have big effects on the accuracy of the results.

Triplicates of each standard dilution were run in this project. The R^2 values calculated for the linear regressions of the standards were not optimal (R^2 was between 0.96 and 0.97) but still stating that the parameters used for calculating the quantities of the samples feature good accuracy.

Yet, these results show that at least five or more repeated measures per standard dilution should be run to improve the accuracy of the linear regression of the standard and thus the sample-quantification.

When choosing how many repeats of every sample-measurement should be done the decision had to be balanced between accuracy and the very limited amount of cDNA sample available, not to mention cost issues. Doing only duplicates of every sample resulted in suboptimal results regarding the standard deviation (mean standard deviation was calculated to be 11.07%) and the results of total copy numbers therefore feature an error at least the magnitude of mean standard deviation.

If - in future projects of the same kind - there is enough sample, it should be considered to run at least triplicates of each sample to minimize standard deviation and thus error of total copy numbers determined.

As shown above the EAAT1 wt copy number was determined by quantification at different sequence positions and subsequent subtraction of the quantification results of either one of the variants. Thus, for the determination of each value for the EAAT1 wt quantification, two different data-sets were used. As stated in section 4.7 this resulted in a 24% difference between the calculated EAAT1 wt mean copy numbers when quantifying at two different positions which of course should have been 0%.

The design of the quantification is obviously not reliable if the aim is to determine an accurate total copy number. This may be explained through the fact that the errors of two different experiments add up when the EAAT1 wt copy numbers were quantified.

Another explanation of this issue may be the RT-PCR efficiency: As any mRNA, the EAAT1 transcript has a long poly-A tail. The poly-T primers used in the RT-PCR will therefore always bind at the poly-A tail whereas the random hexamer primers will bind randomly at different parts of the sequence. As the transcript - in case of EAAT1 wt - is 3983 bases long there will be a considerable proportion of RT-PCR products that do not represent the full length EAAT1 transcript. This proportion of products will also include some that do not contain the exon 3-4 area but still the exon 8-9 area which will result in different total copy numbers when quantifying by means of real-time RT-PCR. Further projects will have to determine the magnitude of this possible source of error.

In terms of total copy numbers reduced accuracy seems to be the major draw back, when designing experiments to quantify splice variants of a gene. Yet, in this project no other design was possible and as shown above, the difference in total copy number means for each of the EAAT1 wt data sets showed the same results when doing the comparison in between case groups, the actual purpose of this project.

As will be shown further down, EAAT1 $\Delta 3$ was detected in very low copy numbers of between twohundred to up to 4000 copies per μg total RNA extract. The exponential phase of the PCR amplification in case of EAAT1 $\Delta 3$ did therefore generally start in the last quarter of the real-time PCR cycling program. Results gained in that phase of the experiment become more and more prone to errors as for example the amplification of primer dimer although this can be seen when carefully checking every single melting curve analysis.

The biggest source of error when quantifying very low copy numbers is that at copy numbers below 100 copies per μg total RNA extract the PCR amplification may fail all together resulting in a lower mean copy number. Changing primer concentrations and sample dilution offer a way to circumvent those errors. In this project those approaches were not applicable as conditions for the quantification of each variant had to be carefully adjusted as to avoid cross-amplification.

When doing comparison on a per-area basis the plotted means in figures 4.12, 4.13 and 4.14 were accompanied by considerable error due to the data not being normally distributed. To gain results with more statistical power, more cases will have to be included in future projects, which should help to get data that is closer to being normally distributed.

5.2 Detection of EAAT1 Splice Variants

The EAAT1 $\Delta 3$ splice variant that previously had only been reported in rat [46] was found to exist in human brain tissue although in very low numbers. No role of this variant is established yet and further research will have to be done to assess possible functions on the transcriptional and protein level. It can be assumed that there are other EAAT1 splice variants, yet they are probably transcribed in such low copy numbers that they were not detected in this project nor would they have any significant effect on the onset or disease severity of AD.

The existence of the previously reported EAAT1 $\Delta 9$ variant in human was confirmed in our samples and makes up a considerable fraction of the EAAT1 wt transcript. It is therefore interesting to examine whether this transcript may act as regulatory mRNA and whether it is actually translated into protein *in vivo*.

5.3 Comparative Analysis of the Transcription Pattern of all EAAT1 Variants in Control and AD Cases

Comparison of brain samples form Control and AD cases

In disease numerous bodily functions such as RNA-transcription and protein expression may be down-regulated. It is therefore uncertain whether the found down regulation of a gene is merely due to general down regulation or is in fact specific for the disease. Numerous studies [78, 79, 80, 81, 74] assessed the possibility to quantify houskeeping genes additionally to the transcript of interest. In theory houskeeping genes are constitutively transcribed at constant levels - if a general down regulation of bodily functions occurs in disease, houskeeping genes will be affected as well and the magnitude of their down regulation may be used as normalization factor for the seen down regulation of the transcript of interest. Preliminary data of our research group confirms that transcription of numerous housekeeping genes is down regulated in AD. In case of Glyceraldehyde 3-phosphate dehydrogenase (GAPDH) this is significant: P=0.04 and r=0.36. The down regulation of EAAT1 transcription in AD has an effect size twice as big (P<0.0001; r=0.64) therefore EAAT1 down regulation is not explained by the general down regulation of gene transcription assessed by GAPDH quantification but is specific for AD.

Yet, the preliminary data also show that GAPDH is intercase variant in AD cases and therefore is not the best candidate to use as normalization factor. Further studies will have to find houskeeping genes that are less intercase variant in AD, being more reliable as normalization factor.

Down Regulation of EAAT1 wt and the Δ3 and Δ9 variants in AD

A significant reduction of the transcripts of all EAAT1 variants (wt, Δ3 and Δ9) was shown for Alzheimer cases. For the transcription of EAAT1 wt and EAAT1 Δ9 reductions of 84% and 80% were observed, respectively. The proximity of those values suggests that there is a general underlying mechanism, that results in the reduction of all EAAT1 variants alike, thus negating the hypothesis that EAAT1 Δ9 transcript or the possibly translated protein are one of the basic causes of AD as

suggested in previous studies [61]. Supporting the theory of a general underlying meachanism is the finding of this project, that there is no significant difference of EAAT1 wt or EAAT1 Δ9 transcription in between more affected areas (inferior frontal and temporal) and less affected areas (posterior motor and occipital pole). If altered EAAT1 transcription and subsequent translation indeed were a major cause instead of a consequence of AD, it would be expected that there are differences in transcription patterns between affected and unaffected areas. Recent publications [47, 33] found EAAT1 reduction in fibroblasts and platelets of AD cases, again supporting the theory of a general mechanism effecting numerous kinds of tissue.

This underlying mechanism may be correlated to APP metabolism which is altered in AD and is seen in connection with negatively effecting the glutamergic system in general [31, 32]. Future studies could therefore aim to examine altered APP metabolism in connection to altered glutamate uptake.

EAAT1 Δ3

The transcription of EAAT1 Δ3, being on average just 0.15% of EAAT1 wt is thought to be such a fractional amount, that it could not possibly have any influence on the onset nor disease severity of Alzheimer's Disease. This becomes especially clear when considering that in control cases the total copy number of EAAT1 3 transcript is about 20-fold higher than in AD and the ratio of EAAT1 wt to EAAT1 Δ3 is not significantly different.

EAAT1 Δ9

The difference seen in EAAT1 Δ proportion of EAAT1 wt in posterior motor and occipital pole areas of AD cases is not thought to have any effect as the total copy number of EAAT1 Δ9 is still significantly higher in the same areas of control cases. Yet, it doesn't rule out the possibility that the EAAT1 Δ9 mRNA plays some role as regulator of EAAT1 wt expression. After all, EATT1 Δ9 mRNA amounts to 26% of EAAT1 wt and it is therefore at least questionable whether its transcription is just an evolutionary dead end or rather has a purpose. Future projects will have to take a look at

that possibility and whether this putative regulation is of the silencing or enhancing kind.

Conclusion

A 40-50% reduction of glutamate uptake in AD has already been reported [28] and the results of this project show, that in case of the glutamate transporter EAAT1 a reduction already takes place on the mRNA level. This reduction is thought to lead to a reduction of EAAT1 expression which will then result in an impaired glutamate uptake system and toxic levels of glutamate, ultimately killing neurons. Further research will have to be done in order to determine whether there are any differences in translation and post-translation of EAAT1 in AD, adding to the effects of reduced transcription. The transcription/translation ratio of EAAT1 is another figure that will have to be assessed - due to numerous RNA/DNA degradation processes that are in action constitutively in cells it is improbable that 1 RNA copy equals 1 protein copy.
Knowing that EAAT1 transcription is reduced in AD will have to go along with looking for reasons for this down-regulation.

Therapy and Early Diagnosis

The knowledge that EAAT1 transcription is reduced in different tissues in AD could be the starting point for the development of a early diagnosis method of AD (though further studies would have to be done as to assess whether EAAT1 reduction is specific for AD or dementia in general): Blood samples could be used to isolate fibroblasts and/or platelets over a course of time to test for progressive reduction of EAAT1.

Independent of the actual cause of EAAT1 reduction gene-therapies could be developed to help increase the level of EAAT1 expression. One theoretical approach would be the cultivation of affected cells (which would have to be taken from each individual that is to be treated) and their transformation with EAAT1 wt containing, promotor-controlled vectors. Those transformed cells could then be re transplanted to AD affected areas in their original donor to and would then transiently express EAAT1

wt, helping to reduce glutamate levels. Developing a method like this would take years so it can be only one of the ways to go to treat reduced glutamate uptake.

Chapter 6

Appendix

Table 6.1: List of Cases

[1]Case numbering was done by the Queensland Brain Bank. In some cases post mortem intervals were not available (n/a).

Case[1]	Age	Sex	Diagnosis	Post Mortem Interval hours:minutes
101	71	female	C	07:45
127	89	male	C	17:00
128	54	female	C	15:45
129	70	female	C	18:00
135	75	female	C	24:26
137	81	female	C	21:26
139	70	male	C	46:10
146	82	female	AD	41:15
148	83	female	C	18:30
158	82	male	C	46:50
162	57	female	C	09:45
172	32	female	C	48:25
175	78	female	C	04:00
177	87	female	AD	35:30
186	61	female	AD	n/a
188	66	female	AD	55:30
189	92	female	AD	n/a
190	79	male	AD	26:20
193	72	male	AD	20:00
196	78	female	AD	n/a
200	82	male	AD	54:55
212	79	male	AD	07:30
214	78	female	AD	07:30

Table 6.2: List of used Primers

Primername	Length (bases)	GC-content (%)	Secondary Structure	Annealing Temperature (^{0}C)	Sequence (5'-3')
EAAT1 CDS FP	25	40.0	none	55.4	ATG ACT AAA AGC AAT GGA GAA GAG C
EAAT1 CDS RP	23	43.5	very weak	54.6	TCT ACA TCT TGG TTT CAC TGT CG
EAAT1 exon 2a FP	21	52.4	none	57.4	CGC ACA CTT TTG GCC AAG AAG
EAAT1 exon 2b FP	21	57.1	very weak	58.4	CAC CGC TGT CAT TGT GGG TAC
EAAT1 exon 4 RP	26	46.2	weak	57.2	TCT TCC CTG ATG CCT TAC TAT CTA GC
EAAT1 exon 3skip4ovlap FP	19	52.6	none	57.1	ACC GCT GTC ATT GTG GGA A
EAAT1 exon 3skip2ovlap FP	19	57.9	none	57.9	CAC CGC TGT CAT TGT GGG A
EAAT1 exon 3skip6ovlap FP	21	52.4	weak	58.1	ACC GCT GTC ATT GTG GGA ATG
EAAT1 exon 3 skip RP	24	45.8	very weak	56.8	CAG CTG TCA CTC GTA CAA TTT TGC
EAAT1 exon 8 FP	22	54.5	weak	57.8	CCT ACC CAT CAC CTT CAA GTG C
EAAT1 exon 8/9 RP	19	57.9	weak	58.3	AGC TGT GGC TGT GAT GCT G
EAAT1 exon 9skip3ovlap RP	16	75.0	weak	58.5	CCG GAG GCG ATC CCT G
EAAT1 exon 9skip2ovlap RP	16	68.8	very weak	58.7	TCC GGA GGC GAT CCC T
EAAT1 exon 10 RP	19	57.9	none	57.5	TAC GTT TGT GGT GGT CCG G
T7 Promoter Primer	20	40.0	weak	47.5	TAA TAC GAC TCA CTA TAG GG
M13 Reverse Primer	18	50.0	very weak	54.4	TGT AAA ACG ACG GCC AGT

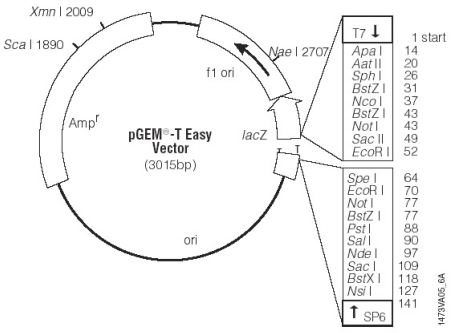

(a) Position of cleavage sites for different restriction enzymes are cited

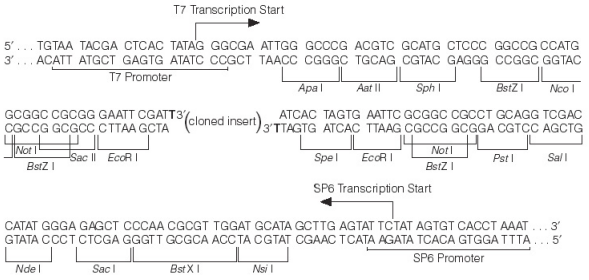

(b) Multiple cloning sequence of the pGEM®-T Easy Vector

Figure 6.1: pGEM®-T Easy Vector circle map and sequence reference points

Chapter 7

Abstract / Zusammenfassung

Today about 24 Million people worldwide suffer from dementia, Alzheimer's Disease accounts for approximately 50-60% of all dementia cases. As the prevalence of dementia grows with increasing age Alzheimer's Disease becomes more and more of an issue for society as the proportion of elderly people increases from year to year.

There are many theoretical approaches to explain the causes and symptoms of Alzheimer's Disease and even though they are at times rather contradictory and have even developed into different schools of thinking this at least states that the disease is the very complex result of many different factors interacting in various ways.

It is well established, that the amino acid glutamate - quantitatively being the most important neurotransmitter in the central nervous system (CNS) - may reach toxic concentrations if not cleared from the synaptic cleft into which it is released during transmittance of action potentials. In Alzheimer's Disease there is strong evidence for a generally impaired glutamate uptake system which in turn is thought to result in toxic levels of the amino acid with the potential to kill off neurons, a typical symptom for the disease.

The excitatory amino acid transporter 1 (EAAT1) belongs to the family of Na^+-dependent glutamate transporter and accounts together with EAAT2 for most of the glutamate uptake in the CNS.

In this project a new splice variant of EAAT1, skipping exon 3 was detected in human brain samples and subsequently called EAAT1 $\Delta 3$, this being the second splice variant found after the recent detection of EAAT1 $\Delta 9$. A method was developed to quantify the transcript of EAAT1 wt, EAAT1 $\Delta 3$ and EAAT1 $\Delta 9$ by means of real-time PCR. Samples were taken from different brain areas of a set of control and AD cases. The areas chosen for examination are affected differently in Alzheimer's Disease, this was used an internal control for the experiments done in this project as to determine whether any effect observed is specific for AD, i.e. AD affected areas or is generally seen in all areas examined.

The results of this project show that EAAT1 $\Delta 3$ is transcribed in very low copy numbers making up a proportion of 0.15% of EAAT1 wt whereas EAAT1 $\Delta 9$ is transcribed in a considerably large proportion of EAAT1 wt of 26.6%.
It was moreover found that all EAAT1 variants are transcribed at significantly lower rates ($P<0.0001$) in AD cases, supporting the theory that EAAT1 protein expression is reduced to a point where glutamate uptake normally mediated by this transporter is impaired. This in turn is thought to result in toxic levels glutamate accounting for neuronal loss in the disease. No area-dependent effects were found, suggesting that the reduction of EAAT1 transcription is rather a result of an underlying general mechanism present in AD.

Further research will have to be done to assess the degree of EAAT1 expression in AD and whether those future findings match with the result of this project.

Zusammenfassung

Zur Zeit leiden ca. 24 Millionen Menschen auf der ganzen Welt unter Demenz, Alzheimer macht dabei 50-60% aller Demenzfälle aus. Da der Anteil der Bevölkerung, der an Demenz leidet, proportional zum Alter zunimmt und der Anteil älterer Menschen in der Gesellschaft von Jahr zu Jahr steigt, wird Alzheimer immer mehr zu einem ernstzunehmenden, gesellschaftlichen Problem.

Es gibt verschiedenste Ansätze, die Gründe und Symptome der Alzheimerschen Krankheit zu erklären. Obwohl diese zum Teil widersprüchlich sind, so macht dies zumindest klar, dass Alzheimer eine sehr komplexe Krankheit darstellt bei der verschiedenste Faktoren in unterschiedlicher Art und Weise zusammenwirken.

Zum Stand der heutigen Forschung ist es etabliert, dass die Aminosäure Glutamat - quantitativ einer der wichtigsten Neurotransmitter im Zentralen Nervensystem (ZNS) - toxische Konzentrationen erreichen kann wenn sie - im Zuge der Übertragung von Aktionspotentialen - nach ihrer Freisetzung nicht aus dem Synaptischen Spalt entfernt wird. Viele Studien haben gezeigt, dass in der Alzheimerschen Krankheit die Glutamataufnahme beeinträchtigt ist, was zu toxischen Konzentrationen von Glutamat und dem daraus folgenden Absterben von Neuronen führt. Dies stellt ein typisches Symptom der Krankheit dar.

Der exitatorische Aminosäuretransporter 1 (EAAT1) gehört zu der Familie der Na^+-abhängigen Glutamattransporter und stellt nach EAAT2 den quantitativ wichtigsten Glutamattransporter im ZNS dar. In diesem Projekt wurde eine bis dahin für den Menschen nicht bekannte EAAT1 Spleißvariante, in der Exon 3 ausgeschnitten wird, nachgewiesen. Diese Variante wurde EAAT1 $\Delta 3$ genannt und stellt damit mit EAAT1 $\Delta 9$ die zweite für EAAT1 nachgewiesene Spleißvariante dar. Eine auf real-time RT-PCR basierende Methode wurde entwickelt, um die Transkripte von EAAT1 wildtyp (EAAT1 wt), EAAT1 $\Delta 3$ und EAAT1 $\Delta 9$ zu quantifizieren. Proben aus verschiedenen Hirnarealen wurden aus einem Set von Kontrollen und Alzheimerfällen bei der Quantifizierung verwendet. Die gewählten Areale sind von der Alzheimerschen Krankheit unterschiedlich stark betroffen. Dies dien-

te als interne Kontrolle für die durchgeführten Experimente und ermöglichte so die Differenzierung zwischen beobachteten Effekten: Nur Effekte die alleinig in von Alzheimer betroffenen Gehirnarealen auftreten, können als spezifisch für die Krankheit angesehen werden.

Die Resultate diese Projektes zeigen, dass EAAT1 $\Delta 3$ in sehr geringer Anzahl transkribiert wird, die nur 0.15% der EAAT1 wt Transkription entspricht. Dahingegen entspricht das EAAT1 $\Delta 9$ Transkript im Durchschnitt 26.6% des EAAT1 wt Transkripts.

Es wurde nachgewiesen, dass die Transkriptionsrate aller EAAT1 Varianten in Alzheimerfällen signifikant reduziert ist ($P<0.0001$). Dies unterstützt die Theorie, dass bei Alzheimerfällen die EAAT1 Proteinexpression stark reduziert und der Glutamattransport, der normalerweise durch diesen Transporter gewährleistet wird, stark eingeschränkt ist. Dies wiederum resultiert in toxisch hohen Glutamatkonzentrationen und damit dem Absterben von Neuronen. Die gefundene Reduktion der EAAT1 Transkription ist nicht spezifisch für Gehirnareale die von Alzheimer betroffen sind, sondern tritt in selbem Maße in nicht von Alzheimer betroffenen Gehirnarealen auf. Daraus lässt sich schließen, dass die Reduktion der EAAT1 Transkription eher ein Resultat eines in der Alzheimerschen Krankheit präsenten, grundlegenden Krankheitsmechanismus ist als deren Ursache.

Weitere Studien werden sich darauf konzentrieren müssen die Expressionsrate von EAAT1 in der Alzheimerschen Krankheit zu determinieren und sie mit den Resultaten dieses Projekts abzugleichen.

Bibliography

[1] Niels C. Danbolt. Glutamate uptake. *Progress in Neurobiology*, 65:1–105, 2001.

[2] Seal RP and Amara SG. A reentrant loop domain in the glutamate carrier EAAT1 participates in substrate binding and translocation. *Neuron*, 21(6):1487–98, 1998.

[3] Möller HJ and Graeber MB. The case described by Alois Alzheimer in 1911. *Eur Arch Psychiatry Clin Neurosci*, 248:111–122, 1998.

[4] Alois Alzheimer. Über eine eigenartige Erkrankung der Hirnrinde. *All. Z. Psychiat.*, pages 146–48, 1907.

[5] Kaj Blenow, Mony J de Leon, and Hendrik Zetterberg. Alzheimer's Disease. *Lancet*, 368:387–403, 2006.

[6] Cleusa P Ferri, Martin Prince, Carol Brayne, Henry Brodaty, Laura Fratiglioni, Mary Ganguli, Kathleen Hall, Kazuo Hasegawa, Hugh Hendrie, Yueqin Huang, Anthony Jorm, Colin Mathers, Paulo R Menezes andElizabeth Rimmer, and Marcia Scazufca. Global prevalence of dementia: a Delphi consensus study. *Lancet*, 366:2112–17, 2005.

[7] Masters CL, Simms G, Weinman NA, Multhaupt G, McDonald BL, and Beyreuther K. Amyloid plaque core protein in Alzheimer disease and Down syndrome. *Proc Natl Acad Sci USA*, 82:4245–9, 1985.

[8] Kang J, Lemaire HG, Unterbeck A, Salbaum JM, Masters CL, Grzeschik KH, Multhaupt G, Beyreuther K, and Muller-Hill B. The precursor of Alzheimer's disease amyloid A4 protein resembles a cell-surface receptor. *Nature*, 325(6106):733–6, 1987.

[9] Buxbaum JD, Liu KN, Luo Y, Slack JL, Stocking KL, Peschon JJ, Johnson RS, Castner BJ, Ceretti DP, and Black RA. Evidence that tumor necrosis factor alpha converting enzyme is involved in regulated alpha-secretase cleavage of the Alzheimer amyloid protein precursor. *J Biol Chem*, 273(43):27765–7, 1998.

[10] Lammich S, Kojro E, Postina R, Gilbert S, Pfeiffer R, Jasionowski M, Haass C, and Fahrenholz F. Constitutive and regulated alpha-secretase cleavage of Alzheimer's amyloid precursor protein by a disintegrin metalloprotease. *Proc Natl Acad Sci USA*, 96:3922–7, 1999.

[11] Sam Gandy. The role of cerebral amyloid β accumulation in common forms of Alzheimer disease. *The Journal of Clinical Investigation*, 115:1121–29, 2005.

[12] Vassar R et al. Beta-secretase cleavage of Alzheimer's amyloid precursor protein by the transmembrane aspartic protease bace. *Science*, 286(5440):735–41, 1999.

[13] Jarrett JT, Berger EP, and Lansbury PT Jr. The carboxy terminus of the beta amyloid protein is critical for the seeding of amyloid formation: implications for the pathogenesis of Alzheimer's disease. *Biochemistry*, 32(18):4693–7, 1993.

[14] Jarrett JT, Berger EP, and Lansbury PT Jr. The C-terminus of the beta protein is critical in amyloidogenesis. *Ann N Y Acad Sci*, 695:144–8, 1993.

[15] Carson JA and Turner AJ. Beta-amyloid catabolism: roles for neprilysin (nep) and other metallopeptidases? *J Neurochem*, 81(1):1–8, 2002.

[16] Hardy J and Selkoe DJ. The amyloid hypothesis of Alzheimer's disease: progress and problems on the road to therapeutics. *Science*, 297(5580), 2002353-6.

[17] Neve RL and Robakis NK. Alzheimer's disease: a re-examination of the amyloid hypothesis. *Trends Neurosci*, 21(1):15–9, 1998.

[18] Arriagada PV, Growdon JH, Hedley-Whyte ET, and Hyman BT. Neurofibrillary tangles but not senile plaques parallel duration and severity of Alzheimer's disease. *Neurology*, 42:631–9, 1992.

[19] Lee HG, Casadesus G, Zhu X, Joseph JA, Perry G, and Smith MA. Perspectives on the amyloid-beta cascade hypothesis. *J Alzheimers Dis*, 6(2):137–45, 2004.

[20] Grundke-Iqbal I, Iqbal K, Tung YC, Quinlan M an Wisniewski HM, and Binder LI. Abnormal phosphorylation of the microtubule-associated protein tau (tau) in alzheimer cytoskeletal pathology. *Proc Natl Acad Sci USA*, 83(13):4913–7, 1986.

[21] Weingarten DW, Lockwood AH, Hwo SY, and Kirschner MW. A protein factor essential for microtubule assembly. *PNAS*, 72:1858–62, 1975.

[22] Iqbal K et al. Tau pathology in Alzheimer disease and other tauopathies. *Biochim Biophys Acta*, 1739:198–210, 2005.

[23] Kahlid Iqbal et al. *Alzheimer Neurofibrillary Degeneration: Significance, Mechanism and Therapeutic Targets*. Ana Aslan.

[24] Olney JW and Ho OL. Brain damage in infant mice following oral intake of glutamate, aspartate or cysteine. *Nature*, 227:609–11, 1970.

[25] Olney JW. Glutamate-induced neuronal necrosis in the infant mouse hypothalamus: an electron microscopic study. *J Neuropathol Exp Neurol*, 30:75–90, 1971.

[26] Olney JW. The toxic effects of glutamate and related compounds in the retina and the brain. *Retina*, 2:341–359, 1982.

[27] Maragakis NJ and Rothstein JD. Glutamate transporters in neurologic disease. *Archives of Neurology*, 58(3):365–70, 2001.

[28] Shi Li et al. Glutamate Transporter Alterations in Alzheimer Disease Are Possibly Associated with Abnormal APP Expression. *Journal of Neuropathology and Experimental Neurology*, 56:901–11, 1997.

[29] Masliah E, Westland CE, Rockenstein EM, Abraham CR, Mallory M, Veinberg I, Sheldon E, and Mucke L. Amyloid precursor proteins protect neurons of transgenic mice against acute and chronic excitotoxic injuries in vivo. *Neuroscience*, 87:135–46, 1997.

[30] Thorns V, Mallory M, Hansen L, and Masliah E. Alterations in glutamate receptor 2/3 subunits and amyloid precursor protein expression during the course of Alzheimer's disease and Lewy body variant. *Acta Neuropathol*, 94(6):539–48, 1997.

[31] Harris ME, Wang Y, Pedigo NW, Hensley K, Butterfield DA, and Carney JM. Amyloid beta peptide (25-35) inhibits Na+-dependent glutamate uptake in rat hippocampal astrocyte cultures. *J Neurochem*, 67(1):277–86, 1996.

[32] Masliah E, Raber J, Alford M, Mallory M, Mattson MP, Yang D, Wong D, and Mucke L. Amyloid protein precursor stimulates excitatory amino acid transport. implications for roles in neuroprotection and pathogenesis. *J Biol Chem*, 273(20):12548–54, 1998.

[33] Chiara P. Zoia, Elena Tagliabue, Valeria Isella, Barbara Begni, Lorenzo Fumagalli, Laura Brighina, Ildebrando Appollonio, Marco Racchi, and Carlo Ferrarese. Fibroblast glutamate transport in aging and in AD: correlations with disease severity. *Neurobiology of Aging*, 26:825–832, 2006.

[34] Goate et al. Segregation of a missense mutation in the amyloid precursor protein gene with familial Alzheimer's disease. *Nature*, 349:704–06, 1991.

[35] Sherrington R, Rogaev EI, and Liang Y et al. Cloning of a gene bearing missense mutations in early-onset familial Alzheimer's disease. *Nature*, 375:754–60, 1995.

[36] Levy-Lahad E, Wasco W, and Poorkaj P et al. Candidate gene for the chromosome 1 familial Alzheimer's disease locus. *Science*, 269:973–77, 1995.

[37] Harvey RJ, Skelton-Robinson M, and Rossor MN. The prevalence and causes of dementia in people under the age of 65 years. *J Neurol Neurosurg Psychiatr*, 74:1206–09, 2003.

[38] Corder EH, Saunders AM, and Strittmatter WJ et al. Gene dose of apolipoprotein E type 4 allele and the risk of Alzheimer's diesease in late onset families. *Science*, 261:921–23, 1993.

[39] Poirier J, Davignon J, Bouthillier D, Kogan S, and Bertrand P Gauthier S. Apolipoprotein E polymorphism and Alzheimer's disease. *Lancet*, 342:697–99, 1993.

[40] Farrer LA, Cupples LA, and et al Haines JL. Effects of age, sex and ethnicity on the association between apolipoprotein E genotype and Alzheimer disease: a meta analysis. *JAMA*, 278:1349–56, 1997.

[41] Miyata M and Smith JD. Apolipoprotein E allele-specific antioxidant activity and effects on cytotoxicity by oxidative insults and beta-amyloid peptides. *NAt. Genet.*, 14:55–61, 1996.

[42] Fonnum F. Glutamate: a neurotransmitter in mammalian brain. *J. Neurochem*, 42:1–11, 1984.

[43] Dingledine R, Borges K, Bowie D, and Traynelis SF. The glutamate receptor ion channels. *Pharmacol Rev*, 51(1):7–61, 1999.

[44] Amara SG and Fontana ACK. Excitatory amino acid transporters: keeping up with glutamate. *Neurochemistry International*, 41:313–318, 2002.

[45] Madl JE and Burgesser K. Adenosine triphosphate depletion reverses sodium-dependent, neuronal uptake of glutamate in rat hippocampal slices. *J Neurosci*, 13(10):4429–44, 1993.

[46] Hugget J, Vaughan-Thomas A, and MAson D. The open reading frame of the Na^+-dependent glutamate transporter GLAST-1 is expressed in bone and a splice variant is of this molecule is expressed in bone and brain. *FEBS Lett*, 485(1):13–8, 2000.

[47] Chiara Zoia, Tiziana Cogliati, Elena Tagliabue, Guido Cavaletti, Gessica Salaa nd Gloria Galimberti, Ilaria Rivolta, Vincenzo Rossi, Lodovico Frattola, and Carlo Ferrarese. Glutamate transporters in platelets: EAAT1 decrease in aging and in Alzheimer's disease. *Neurobiology of Aging*, 25:149–157, 2004.

[48] Lehre KP et al. Differential expression of two glial glutamate transporters in the rat brain: quantitative and immunocytochemical observations. *J Neurosci*, 15:1835–53, 1995.

[49] Gammelsaeter R, Danbolt NC, Storm-Mathisen J, and Grundersen V. Glutamate transport proteins in the rat panvreatic islets of Langerhans. *J. Neurochem.*, 73:S99D, 1999.

[50] Haugeto O et al. Brain glutamate transporter proteins form homomultimers. *J Biol Chem*, 271(44):27715–22, 1996.

[51] Kanai Y and Hediger MA. Primary structure and functional characterization of a high-affinity glutamate transporter. *Nature*, 360(6403):467–71, 1992.

[52] Kugler P and Schmitt A. Glutamate transporter EAAC1 is expressed in neurons and glial cells in the rat nervous system. *Glia*, 27(2):129–42, 1999.

[53] Arriza JL, Eliasof S, Kavanaugh MP, and Amara SG. Excitatory amino acid transporter 5, a retinal glutamate transporter coupled to a chloride conductance. *Proc Acad Natl Sci USA*, 94:4155–60, 1997.

[54] Lipton SA and Rosenberg PA. Excitatory amino acids as a final common pathway for neurologic disorders. *N Engl J Med*, 330(9):613–22, 1994.

[55] Volterra A, Trotti D, and Racaqni G. Glutamate uptake is inhibited by arachidonic acid and oxygen radicals via two distinct and additive mechanisms. *Mol Pharmacol*, 46(5):986–92, 1994.

[56] Bannai S. Exchange of cystine and glutamate across plasma membrane of human fibroblasts. *J Biol Chem*, 261(5):2256–63, 1986.

[57] www.ensembl.org. Ensg00000079215, 2006.

[58] www.ncbi.nlm.nih.gov. Nm004172. 2006.

[59] Seal RP, Leighton BH, and Amara SG. A model for the topology of excitatory amino acid transporters determined by the extracellular accessability of substituted cysteines. *Neuron*, 25:695–706, 2000.

[60] Macnab LT, Williams SM, and Pow DV. Expression of the exon 3 skipping form of GLAST, GLAST1a, in brain and retina. *NeuroReport*, 00:1–4, 2006.

[61] Vallejo-Illarramendi A, Domercq M, and Matute C. A novel alternative splicing form of excitatory amino acid transporter 1 is a negative regulator of glutamate uptake. *Journal of Neurochemistry*, 95:341–48, 2005.

[62] Honiq LS, Chambliss DD, Bigio EH, Carroll SL, and Elliot JL. Glutamate transporter EAAT2 splice variants occur not only in ALS, but also in AD and controls. *Neurology*, 55(8):1082–8, 2000.

[63] Walton HS, Gebhardt FM, Innes DJ, and Dodd PR. Analysis of multiple exon-skipping mRNA splice variants using SYBR Green real-time RT-PCR. *J Neurosci Methods*, Epub ahead of print, 2006.

[64] Eliezer Masliah, Michael Alford, Margaret Mallory, Edward Rockenstein, Dieder Moechars, and Fred Van Leuven. Abnormal glutamate transport function in mutant amyloid precursor protein transgenic mice. *Experimental Neurology*, 163:381–87, 2000.

[65] Watase K et al. Motor discoordination and increased susceptibility to cerebelar injury in GLAST mutant mice. *J Neurosci*, 10:976–88, 1998.

[66] Scott HL, Pow DV, Tannenberg AE, and Dodd PR. Aberrant expression of the glutamate transporter excitatory amino acid transporter 1 (EAAT1) in Alzheimer's disease. *J Neurosci*, 229(3):RC206, 2002.

[67] Sigma. www.sigmaaldrich.com, 2006.

[68] Sambrook, Fritsch, and Maniatis. *Molecular Cloning - A Laboratory Manual*, volume 1 to 3. Cold Spring Harbor Laboratory Press, 2nd edition, 1989.

[69] Ellington A adn Pollard JD. Purification of Oligonucleotides Using Denaturing Polyacrylamide Gel Electrophoresis. *Current Protocols in Molecular Biology*, pages 2.12.1–2.12.7, 1998.

[70] Invitrogen. *PureLink^{TM} HiPure Plasmid DNA Purification Kits*. Invitrogen^{TM} life technologies, March 2005.

[71] Promega. *Wizard® PCR Clean up System*. Promega Corporation, 2005.

[72] Promega. *pGEM®-T and pGEM®-T Easy Vector Systems*. Promega Coorperation, 2005.

[73] F. Sanger, Nicklen, and Coulson. DNA Sequencing with chain-terminating inhibitors. *Proceedings of the National Academy of Sciences*, 74:5463–7, 1977.

[74] Bustin SA. Absolute quantification of mRNA using real-time reverse transcription polymerase chain reaction assays. *Journal of Molecular Endocrinology*, pages 169–193, 2000.

[75] Morrison TB et al. Quantification of low-copy transcripts by continuous SYBR Green I monitoring during amplification. *Biotechniques*, 24(6):954–8, 1998.

[76] Biosystems A. Creating standard curves with genomic DNA or plasmid DNA, 2003.

[77] Pfaffel MW, Tichopad A, Prgomet C, and Neuvians TP. Determination of novel stable housekeeping genes, differentially regulated target genes and sample integrity: bestkeeper-excel-based tool using pair-wise correlations. *Biotechnol Lett*, 26:509–15, 2004.

[78] X. Sun, V. Beglopoulos, M. P. Mattson, and J. Shen. Hippocampal spatial memory impairments caused by the familial alzheimer's disease-linked presenilin 1 m146v mutation. *Neurodegener Dis*, 2(1):6–15, 2005. 1660-2854 (Print) Journal Article Research Support, N.I.H., Extramural.

[79] P. Preece and N. J. Cairns. Quantifying mrna in postmortem human brain: influence of gender, age at death, postmortem interval, brain ph, agonal state and inter-lobe mrna variance. *Brain Res Mol Brain Res*, 118(1-2):60–71, 2003. 0169-328X (Print) Journal Article.

[80] R. V. Gutala and P. H. Reddy. The use of real-time pcr analysis in a gene expression study of alzheimer's disease post-mortem brains. *J Neurosci Methods*, 132(1):101–7, 2004. 0165-0270 (Print) Comparative Study Journal Article Research Support, Non-U.S. Gov't Research Support, U.S. Gov't, P.H.S.

[81] L. Emilsson, P. Saetre, and E. Jazin. Alzheimer's disease: mrna expression profiles of multiple patients show alterations of genes involved with calcium signaling. *Neurobiol Dis*, 21(3):618–25, 2006. 0969-9961 (Print) Journal Article Research Support, Non-U.S. Gov't.